

UNIVERSITY OF OKLAHOMA  
GRADUATE COLLEGE

INFRARED THERMAL IMAGING-BASED THERMAL DIFFUSIVITY MEASUREMENT  
USING ANGSTROM METHOD

A THESIS  
SUBMITTED TO THE GRADUATE FACULTY  
in partial fulfillment of the requirements for the  
Degree of  
MASTER OF SCIENCE

By  
BRADLEY D. WOOLERY  
Norman, Oklahoma  
2021

INFRARED THERMAL IMAGING-BASED THERMAL DIFFUSIVITY MEASUREMENT  
USING ANGSTROM METHOD

A THESIS APPROVED FOR THE  
SCHOOL OF AEROSPACE AND MECHANICAL ENGINEERING

BY THE COMMITTEE CONSISTING OF

Dr. Jivtesh Garg, Chair

Dr. Hamidreza Shabgard

Dr. Jie Cai

© Copyright by BRADLEY D. WOOLERY 2021

All Rights Reserved.

## **Acknowledgements**

Completing this thesis and obtaining my master's degree in mechanical engineering here at the University of Oklahoma would not have been possible without a whole host of people being willing to help me at every step along the way. First and foremost, thanks to my advisor and committee chair, Dr. Jivtesh Garg, for the ideation, input, initial steps taken, and help on my thesis research, and for his patience in teaching me the principles behind the experimental setups in the laboratory. Also, thanks to Dr. Jie Cai and Dr. Hamidreza Shabgard for agreeing to be a part of my thesis committee and oversee my thesis defense. In addition to these, I am thankful for the help from Fatema Tarranum in explaining the prior method from which this new method was developed, and for the initial steps she took to get this project off the ground by building the first sample stage and taking steps to test out the initial idea. Thanks to Swapneel Danayat for collaborating with me and contributing some material as samples with which to test out my experimental setup. Thanks to Dr. Christopher Dalton for his helpful comments on my research and pointing me to the prior work he completed with an infrared camera as part of his dissertation, which came in handy to solve a problem I was having with my experimental setup. Thanks to everyone involved with the Sooner Off-Road team for being part of an experience which gave me much of the practical experience and knowledge required to get through classes and research. Many thanks to all faculty and staff in the Gallogly College of Engineering and the School of Aerospace and Mechanical Engineering for everything they have done to create a good educational environment. And finally, thanks to all of my family who has supported me in this endeavor, particularly my wife, Savannah Woolery, who has given limitless encouragement and support. I could not have made it here without all of you, so thank you all.

# Table of Contents

Acknowledgements.....	iv
Table of Contents.....	v
List of Figures.....	viii
Abstract.....	xi
Chapter 1: Introduction.....	1
1.1 Background.....	1
1.2 Purpose.....	2
1.3 Angstrom Method.....	2
1.3.1 Practical process.....	2
1.3.2 Analysis process.....	4
1.4 Prior measurement technique.....	5
1.5 Goals.....	6
1.5.1 Lower cost.....	6
1.5.2 Accuracy.....	6
1.5.3 Reliability.....	7
1.5.4 Ease of Use.....	7
1.5.5 Reduced sample preparation requirements.....	7
1.6 Vacuum chamber.....	7

Chapter 2: Angstrom Method based on Infrared Imaging .....	10
2.1 Material samples .....	11
2.1.1 Plane heater application .....	12
2.1.2 Surface emissivity modification .....	13
2.2 Infrared camera .....	14
2.2.1 Vacuum chamber viewport for camera.....	16
2.2.2 Software used to read data .....	17
2.3 “Blast shield” creation.....	18
2.4 Determining measurement point placement.....	19
Chapter 3: Sample Stage Development .....	22
3.1 Reference datum.....	23
3.2 Layback angle .....	25
3.3 3D printing .....	27
3.3.1 Designing for 3D printing.....	27
3.3.2 Additional design features .....	28
Chapter 4: Sample Measurement .....	32
4.1 Calibration of surface emissivity.....	32
4.2 Steps completed for each measurement .....	35
4.3 Point locator spreadsheet.....	36

Chapter 5: Data Analysis .....	39
5.1 Curve fitting .....	42
5.2 Automation of Analysis .....	46
Chapter 6: Results .....	47
6.1 Data obtained.....	47
6.1.1 Polypropylene .....	47
6.1.2 Expanding to other materials .....	49
6.1.3 Polylactic Acid.....	50
6.1.4 Graphene-thermoplastic nanocomposite.....	55
6.2 Agreement with published values, other methods .....	59
6.2.1 Polypropylene samples .....	59
6.2.2 PLA samples .....	61
6.3 Sources of error .....	61
Chapter 7: Conclusion and Remarks.....	64
7.1 Reliability of method.....	64
7.2 Future applications of the method.....	64
7.3 Future improvements.....	65
References.....	66
Appendix.....	68

## List of Figures

Figure 1 - Example of a material sample used in Angstrom method analysis.....	4
Figure 2 - Diagram of Angstrom method parameters.....	5
Figure 3 - Vacuum chamber, connected to vacuum pump .....	8
Figure 4 - Pfeiffer HiCube 80 Eco vacuum pump .....	9
Figure 5 - Experimental setup (left to right): function generator, vacuum chamber, infrared camera, desktop computer .....	10
Figure 6 - Sample dimensions (mm).....	11
Figure 7 - PLA samples with plane heaters applied .....	12
Figure 8 - Two fully prepared polypropylene samples loaded onto sample stage MK3 .....	14
Figure 9 - FLIR camera, lens, and adjustable platform .....	15
Figure 10 – Viewport lens with coating.....	16
Figure 11 - FLIR ResearchIR Max software, representative image .....	18
Figure 12 - Blast Shield, which sits around the camera and viewport.....	19
Figure 13 - Four points set up for data collection (test F) .....	20
Figure 14 - Six points set up for data collection (test K) .....	21
Figure 15 - Initial sample stage design, made by Fatema.....	22
Figure 16 - Final sample stage design MK3 .....	23
Figure 17 - Reference datum on sample stage MK3.....	24



Figure 18 - Sample Stage MK2, with no layback angle .....	26
Figure 19 - Sample Stage MK3, with 30° layback angle and PLA sample blank in place .....	26
Figure 20 - Print layout of Sample Stage (MK2 pictured).....	28
Figure 21 - Integrated clamp closeup on MK2 model of sample stage, with samples in place....	29
Figure 22 - Integrated clamps of MK3 sample stage, side profile shown on SOLIDWORKS CAD model.....	30
Figure 23 - Sample stage mounted inside vacuum chamber.....	31
Figure 24 – Back side of calibration plate, with heater shown.....	33
Figure 25 - Front side of calibration plate, with surface coating and thermocouple mounting shown .....	33
Figure 26 - Comparison of data from Calibration of Infrared Camera.....	35
Figure 27 – Measured points, to take coordinates of in camera feed and input to spreadsheet....	37
Figure 28 - Cursor placement locations output, based on measured points.....	38
Figure 29 - Combined Data graph .....	40
Figure 30 - Narrow Data graph.....	41
Figure 31 - Curve approximation - Cursor 3 .....	43
Figure 32 - Curve approximation - Cursor 2 .....	43
Figure 33 - Curve approximation - Cursor 1 .....	44
Figure 34 - Combined Approximations .....	45
Figure 35 - Thermal Diffusivity of Polypropylene.....	48

Figure 36 - PLA samples pictured in Cura slicer software, with the red arrow demonstrating direction of alignment in layers ..... 51

Figure 37 - Thermal diffusivity of PLA 3D printed samples at different layer angles..... 52

Figure 38 - Temperature variations on surface of 0° (longitudinal) PLA sample (test L)..... 53

Figure 39 - Cursors placed over variable temperature surface (Test L) ..... 53

Figure 40 - Cursor placement over variable temperature surface of 90° sample (test M)..... 54

Figure 41 - Cursor placement over variable temperature surface of 45° sample (test I) ..... 55

Figure 42 - Graphene/polymer nanocomposite samples, defects showing..... 56

Figure 43 - Graphene/polymer nanocomposite samples, same as above but overexposed to show the extent of the defects. .... 57

Figure 44 – Thermal Diffusivity of Graphene/Polymer nanocomposite ..... 58

Figure 45 - Curve fit of polypropylene thermal diffusivity data from Zhang and Fujii [14] with experimentally determined and laser flash analysis values overlaid ..... 60

## Abstract

Characterizing the thermal diffusivity of materials is a vital step in the creation of new polymer nanocomposites. Determining the in-plane thermal diffusivity as compared to the through-plane thermal diffusivity may show the effectiveness of a material for a given application. Through experimentation and trial of various materials, an experimental setup is developed for use with Angstrom method to determine in-plane thermal diffusivity of samples using an infrared (thermography) camera with data gathering capabilities. Development of various elements of the experimental setup—such as a 3D printed stage to hold samples—is discussed, along with an explanation of data analysis methods. Data gathered showed that the setup yielded accurate thermal diffusivity of polypropylene samples ( $\sim 0.164 \text{ mm}^2/\text{s}$  at approximately  $33 \text{ }^\circ\text{C}$ ) within  $\sim 10\%$  of published values at that temperature. These results were further validated through laser flash analysis. 3D printed PLA samples were also characterized, and lessons learned from those measurements are discussed along with implications for the experimental technique.

# Chapter 1: Introduction

## 1.1 Background

Polymers are used in the construction of many consumer and industrial products, with increasing popularity, and are very versatile and adaptable to different shapes and designs. As usage of polymers grows, more and more applications are being developed which require polymers to have improved properties such as higher strength, resistance to degradation, or increased heat conduction. For example, in the age of modern integrated electronics, electronic components are being built into many different products. Waste heat is generated by many of these electronic components, and this waste heat is best carried away from the heat-producing components for the sake of longevity. However, many of these electronics are encased in polymer shells, and polymers are generally not very thermally conductive in their purest forms. This can be a benefit in some cases, but a significant downside in others, such as the situation in this example where efficient heat dissipation is needed.

As new materials are being created in the lab to fill this void and produce polymer materials with higher thermal conductivity, the materials must be characterized, and thermal properties extracted to allow proof of their effectiveness for thermal applications. Anisotropic materials make thermal conductivity characterization more challenging. While through-plane thermal conductivity can easily and quickly be determined using methods such as laser flash analysis, in-plane thermal conductivity can be more difficult. However, it is necessary to determine this in-plane thermal conductivity when testing directional materials such as nanocomposites with aligned particles or composites with directional fibers.

## **1.2 Purpose**

The purpose of the research conducted for this thesis was to develop a method in which the in-plane thermal diffusivity of materials with relatively low thermal diffusivity (primarily polymer samples) could be measured with relatively low cost, high accuracy, reliability, ease of use, and significantly reduced sample preparation requirements. Once the in-plane thermal diffusivity is obtained, the in-plane thermal conductivity can be obtained with relative ease. The method used to achieve this measurement is explained, and these goals are reiterated with more detail in the following sections.

## **1.3 Angstrom Method**

The Angstrom method for determining in-plane thermal diffusivity is derived and detailed in many publications, including the thesis work of Fatema Tarranum, a fellow researcher in our lab who previously worked extensively with Angstrom method in the characterization of various conductive materials [1], [2]. Angstrom method will not be derived in detail here, but a short summary is provided to give the reader necessary information for the content of this thesis. The practical process of setting up a measurement is discussed, followed by the analysis and theory behind the method.

### ***1.3.1 Practical process***

The practical process for using Angstrom method to determine thermal diffusivity in an experimental setup is explained in the following:

- Heat conduction occurs as thermal energy travels through a piece of material. Angstrom method centers around a piece of material to be tested. The cross-sectional area of the sample must be constant along its length.
- A plane heater is placed directly in the middle of the sample, positioned such that the entire cross-sectional plane is heated at once, with the same heat flux across the plane, when the heater is powered.
- Convection around the sample or piece of material is prevented through the application of a vacuum. The goal of this is to restrict thermal energy transfer through every method except conduction.
- Once the material is prepared, heat is applied through the plane heater in a periodic fashion – specifically a sine wave in this application. A periodic heat wave travels through the material at a rate related to the thermal diffusivity of the material.
- Measurements over time are taken at two points within the material, set a fixed distance apart, allowing the temperature fluctuations at each point with respect to time to be measured. These measurements are synchronized to each other with respect to time, and the measurement taken at a point further away from the heater lags the other.
- Finally, the system's transient state stops changing after a while (~100 minutes in this application), and a section of data from both points is recorded.

An image of an experimental sample is placed below (Figure 1) to provide an example of what a typical setup for low-conductivity materials may look like. This sample is shown with an integrated plane heater and thermocouples placed at specific points along its centerline to measure thermal diffusivity.

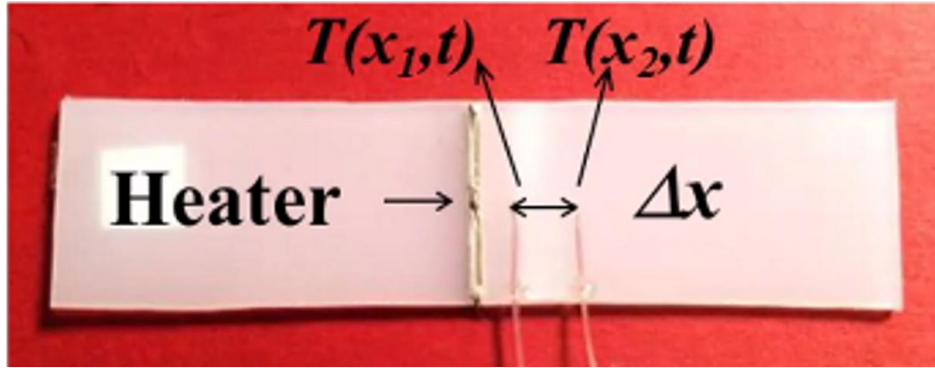


Figure 1 - Example of a material sample used in Angstrom method analysis

### 1.3.2 Analysis process

Data obtained from the two points measured in the experimental setup described in the previous section gives two sinusoidal curves, each one representing the temperature at the specified point as a function of time. These curves (see Figure 2 for an example) are analyzed to determine three factors: amplitude of the periodic temperature wave at point 1 ( $A_1$ ), amplitude of the periodic temperature wave at point 2 ( $A_2$ ), and the phase shift between the two waves ( $\Delta t$ ). These factors, along with the measurement of the distance between the two points ( $\Delta x$ ), are put into Equation 1, which is the final equation in the derivation of Angstrom method, and thermal diffusivity ( $\alpha$ ) is calculated.

Equation 1 - Thermal Diffusivity

$$\alpha = \frac{\Delta x^2}{2\Delta t \ln \frac{A_1}{A_2}}$$

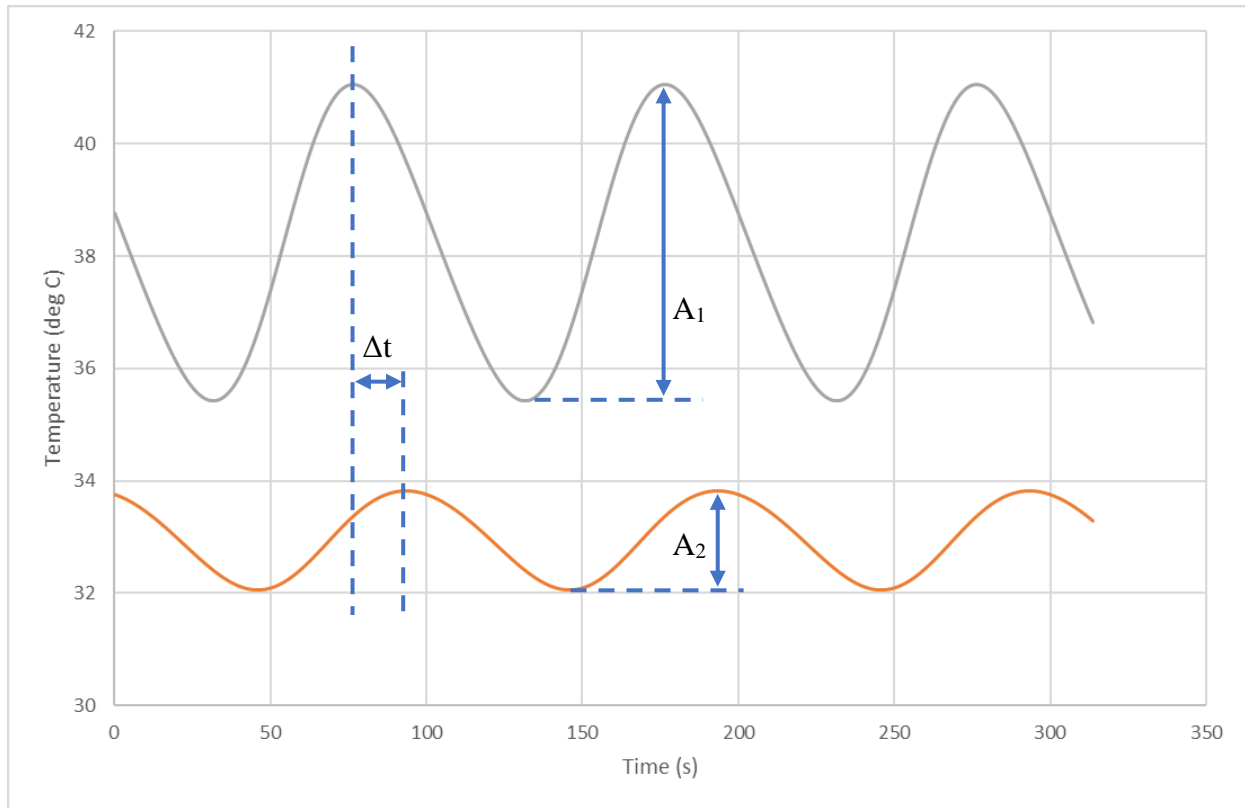


Figure 2 - Diagram of Angstrom method parameters

#### 1.4 Prior measurement technique

The experimental setup (based on Angstrom method) used to measure in-plane thermal conductivity of materials previously in our lab was similar in construction to the new method developed here, apart from the sample preparation and temperature measurement device. In the prior method, samples were prepared with an integrated plane heater in the center of each long rectangular sample; this step is still the same. However, in the samples used for this prior method, it was required to drill tiny holes at the measurement locations (2 and 6mm from the edge of the plane heater on each side) and insert thermocouples into the sample. These thermocouples were affixed to each individual sample and used to measure the temperature at each of the four points.



While this technique was effective in gathering accurate and precise data, the sample preparation process is arduous because of the small holes that must be drilled with precision, and costs of the thermocouples add up quickly.

## **1.5 Goals**

The purpose of developing this new method of characterizing thermal diffusivity is to make improvements over previous methods. The goals for these improvements are detailed below.

### ***1.5.1 Lower cost***

Adding high-accuracy thermocouples to each sample is a cost which adds up very quickly over time, since each sample requires at least two (usually four) thermocouples to be attached and these thermocouples are not reusable. The new method should ideally make use of a temperature reading device which is fully reusable and therefore eliminates thermocouples – reducing costs over time.

### ***1.5.2 Accuracy***

Since thermocouples are inserted into the center of the sample in the prior method, the thermal conductivity through the area where the tip of a thermocouple is present is different from the surrounding material. While the change in thermal conductivity at that point is reduced by selecting and using small thermocouples for the measurement, the effects are still present and become more apparent in thinner samples. Ideally, the new method would have an accuracy close to that of the previous method and produce comparable results. Results should match published values and values obtained using other methods. The new method is based on use of infrared imaging for measurement of temperatures for thermal conductivity measurements.

### ***1.5.3 Reliability***

The improved method must provide reliable results which are consistent and not affected by minute changes in the experimental setup. Any issues with reliability due to the camera setup should be eliminated or reduced as much as possible.

### ***1.5.4 Ease of Use***

The method should be easy to use by researchers in the laboratory. Time spent preparing samples, gathering data, and analyzing data should be reduced whenever possible.

### ***1.5.5 Reduced sample preparation requirements***

Since thermocouples do not need to be added to each sample, several steps of sample preparation are cut out of the process. Thermocouple locations do not need to be marked out in advance, holes do not need to be drilled into the sample, and thermocouples do not need to be adhered in those holes. Not having to deal with any of these thermocouple-related steps speeds the sample preparation process significantly; preparation time saved per sample is estimated at approximately 20 minutes. It also reduces handling time of the samples, which in turn reduces damage and loss of samples, since the heater wires are fragile and susceptible to breakage.

## **1.6 Vacuum chamber**

To properly measure the thermal diffusivity of a material, the primary method of heat transfer must be conduction; the effects of radiation and convection must be limited as much as possible. While radiative heat transfer is difficult to control, convection can easily be reduced by removing the convective medium – in this case, the air around the sample. Evacuating as much of the air from

the chamber as possible is thus very important to the measurement of thermal diffusivity in measurements taking place over a long time such as those required by Angstrom method.

A steel vacuum chamber is sealed with the samples inside, with only a couple of wires running into the otherwise sealed chamber for the purpose of heating the samples. For this research, the chamber from the previous method was reused with slight modifications (detailed further on) to allow for the infrared camera to operate correctly. To achieve very low pressures within the vacuum chamber, a turbomolecular vacuum pump (Pfeiffer Vacuum HiCube 80 Eco) is used to evacuate almost all the air from the chamber. Using this turbine vacuum pump, an absolute vacuum pressure of 35-40 mTorr is achieved within the chamber. The vacuum chamber and vacuum pump used in this application can be seen below in Figure 3 and Figure 4.



*Figure 3 - Vacuum chamber, connected to vacuum pump*



*Figure 4 - Pfeiffer HiCube 80 Eco vacuum pump*

## Chapter 2: Angstrom Method based on Infrared Imaging

Angstrom method as described in Chapter 1 forms the basis for the development of a new technique to measure thermal diffusivity. Rather than measure temperature at points along the sample using thermocouples, an infrared camera is set up to read the temperature at specific points along the surface of the sample. This change from thermocouples to infrared camera allows many improvements to be made to the process of measuring in-plane thermal diffusivity, but also requires several changes from the prior method and involves unique difficulties which must be accounted for. The general setup consists of a vacuum chamber which contains samples mounted on a stage, an adjustable infrared camera pointed at those samples, a function generator to supply a sinusoidal heat wave to the samples, a vacuum pump, and a computer to process the visual feed from the camera and pull the data streams of specific points out of it.



*Figure 5 - Experimental setup (left to right): function generator, vacuum chamber, infrared camera, desktop computer*

## 2.1 Material samples

To examine a given material with the selected method, a sample must be created of the material. The sample should be of a constant, thin thickness (0.5-2mm) and have a constant width to ensure that variations in width do not change the rate of heat diffusion. Additionally, the design of the apparatus to hold these samples and the vacuum chamber itself both pose some limitations on the sample dimensions. From these limitations, an ideal sample size is derived, though there is significant allowance for variation in sample sizes. An ideal sample is between 50–75 mm in length, with 50.8 mm (2 inches) being a good length for the setup. Thickness, again, should be under 2 mm but have enough rigidity to support its own weight without deformation (a minimum of 0.5 mm thickness is suggested, though sometimes thinner samples will work). Width (or height, as shown in the diagram) of the sample should be constant, with a dimension of 10–12 mm suggested. The center slot shown is for application of the plane heater, discussed in the next section.

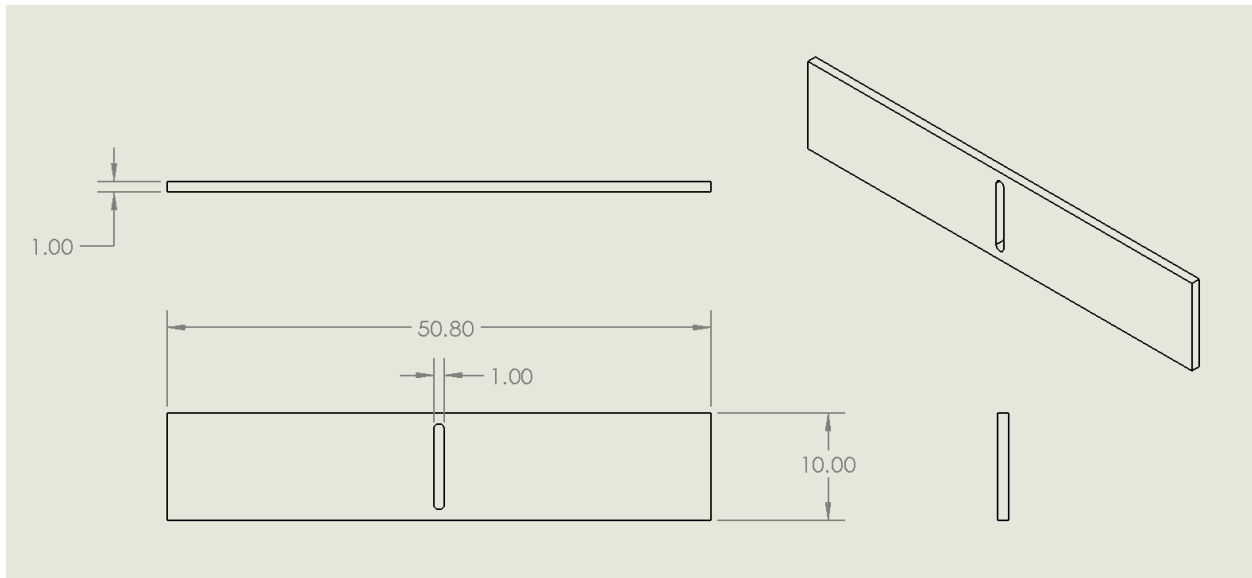


*Figure 6 - Sample dimensions (mm)*

### ***2.1.1 Plane heater application***

To generate a sinusoidal heat wave through the material sample, a plane heater must be applied at the center of each sample as a resistive heater. To ensure the heat is as close to constant through the thickness as possible, a slot is cut in each sample (approximately 1 mm wide, leaving ~1 mm on either end to hold the sample together) and a thin heater wire is wrapped through the sample (AWG 40, with a resistance of 67.4  $\Omega$ /ft). This heater wire is then enveloped in thermal epoxy (Arctic Silver Thermal Adhesive) which fills the rest of the slot and serves to conduct the heat from the wire out to the sample material in an even manner. The thermal epoxy used has a very high thermal conductivity relative to a base polymer material because it is approximately 62-65% “micronized silver” by weight [3]. This allows the heat to be spread more evenly and completely across the central plane heater and therefore the heat wave is more even across the surface as it pushes out toward the extremities of the sample. An image of PLA samples with heaters applied can be seen in Figure 7.

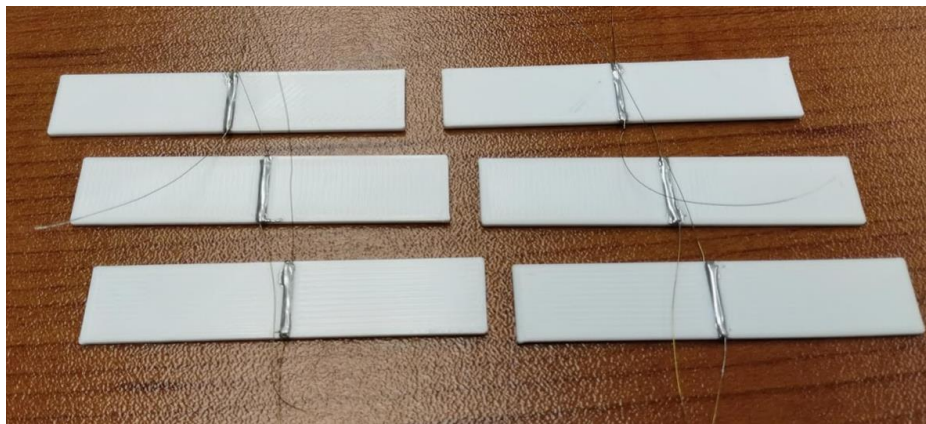


*Figure 7 - PLA samples with plane heaters applied*

### ***2.1.2 Surface emissivity modification***

Samples which are intended to be examined using the infrared camera and Angstrom method system developed in this research may have a variety of surface finishes and colors, if the surface is relatively smooth and the sample is planar. However, to ensure the system is accurately reading temperature at the selected measurement points, the samples should all be coated with a thin layer of graphite paint to ensure the surface emissivity is known and constant across the surface. For this research, a graphite “dry lubricant” spray (DGF 123 Graphite Film Lubricant) was selected because it creates a very thin coating of pure graphite on the surface of the samples which reduces reflectivity by adding a matte finish, and makes the surface emissivity nearly 1.0—close to ideal. See Figure 8 for an example of coated samples. While graphite conducts heat well, a sample is thick enough to make the effect of the graphite on thermal conductivity negligible [4].



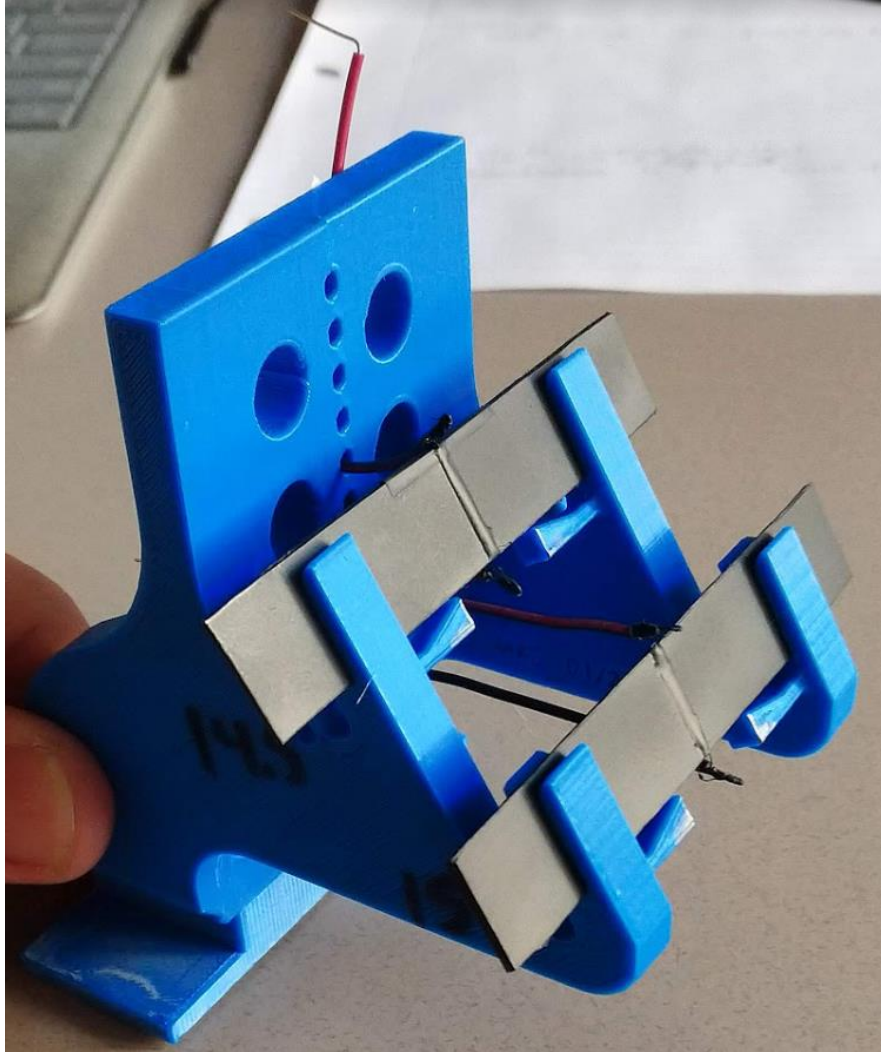


*Figure 8 - Two fully prepared polypropylene samples loaded onto sample stage MK3*

## **2.2 Infrared camera**

The camera selected for this application is a FLIR A325sc thermography camera, which is a laboratory-focused model of infrared camera intended for fixed-mount applications such as this one [5]. It features high frame rates and a high resolution (320x240 pixels at 30 frames/second) for quality data collection, and relies on a separate computer for data collection, processing, and

storage. The camera is fitted with a FLIR T197215 Close-up lens, which allows for 4x zoom focus on the sample from a working distance of 79mm away [6]. This lens allows the camera to be zoomed in enough to get an accurate reading at points close together on the surface; in other words, the closeness of the camera using the selected lens allows for a higher resolution per a given unit length. The camera is mounted on a height-adjustable platform and on a slider which allows focus to be adjusted with precision; these adjustments, in addition to the fact that the camera platform is not fixed to the table, allow for three axes of adjustment in camera placement. Camera, lens, and platform are pictured in Figure 9.

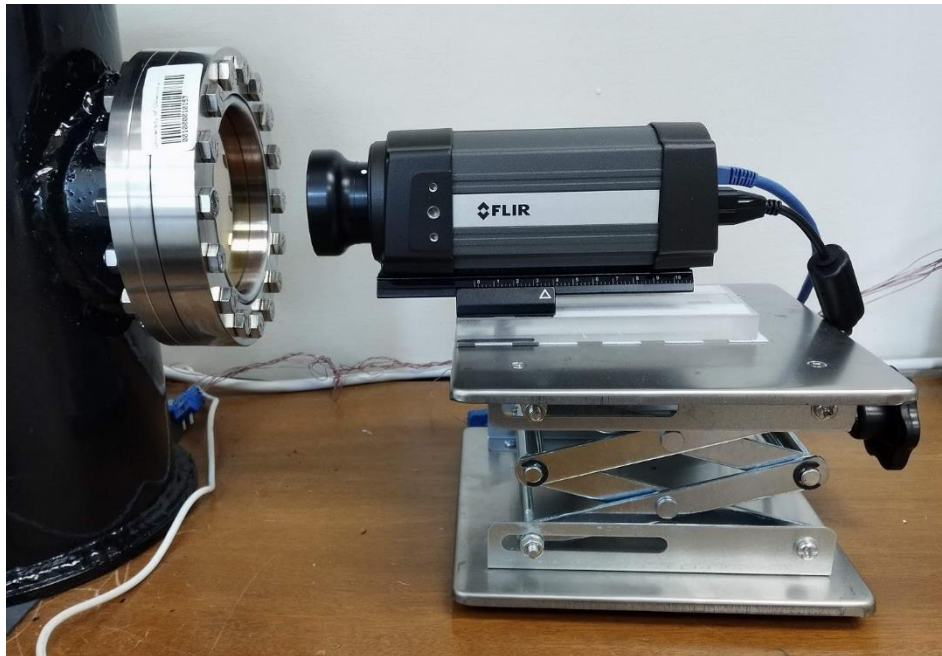


*Figure 9 - FLIR camera, lens, and adjustable platform*

### ***2.2.1 Vacuum chamber viewport for camera***

A zinc selenide (ZnSe) window viewport with antireflective coatings was added to the side of the vacuum chamber to allow the infrared camera to “see” the sample and pull temperature profile data from it. This viewport, a Torr Scientific Zinc Selenide Zero Length viewport, was specifically selected to be capable of handling very strong vacuum pressures, while the material and additional coating reduces reflectivity and helps make the lens of the viewport “invisible” to the infrared camera [7]. This coating specifically helps prevent external heat sources from reflecting off the viewport and into the camera lens, and allows all infrared radiation from inside the chamber to transmit through the window to the outside [8].

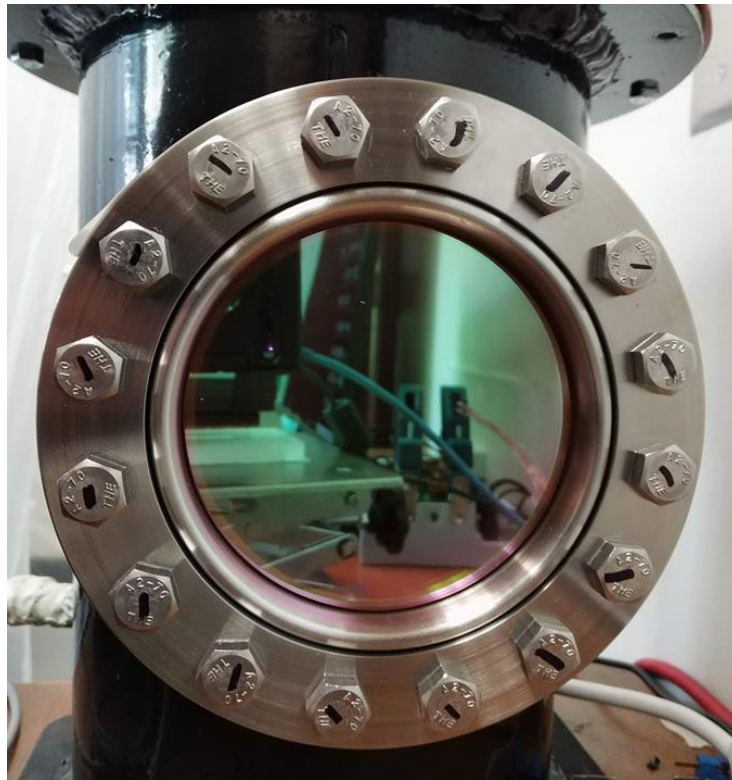


*Figure 10 – Viewport lens with coating*

### ***2.2.2 Software used to read data***

FLIR ResearchIR Max is the software bundled with the FLIR infrared camera selected for this application, and it has been used in this experimental setup to gather data from the infrared camera. Within the software, a live camera feed is presented to the user with a scaled color gradient representing temperature of the surface being inspected. Different color schemes can be selected to show the temperature gradient in different ways. Much of the software is visually driven, since it is a live feed from the camera sensor, but various analysis tools are available; for example, one can use these tools to pull plots of data from specific points within the image. Measurement points are named “points of interest” (POIs) or “cursors” in the FLIR ResearchIR software. These measurement points within the camera feed are called “measurement points” or “cursors” interchangeably herein. In Figure 11, the cursors can be seen on the image, though they are not yet placed in their correct locations on the sample to be tested. A temporal plot for each cursor can also be seen on the right side of the screen.

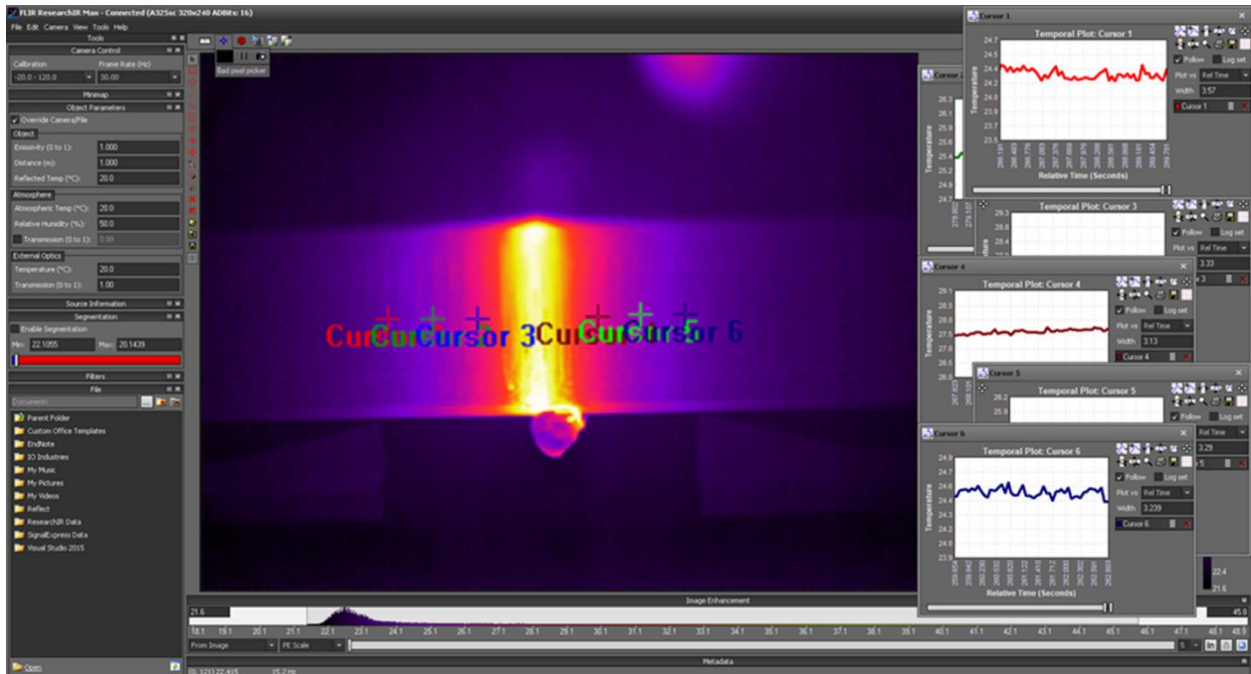


Figure 11 - FLIR ResearchIR Max software, representative image

### 2.3 “Blast shield” creation

A polycarbonate shield was constructed to cover the infrared camera, the camera mounting stand, and the glass viewport in the side of the vacuum chamber (Figure 12). In addition to protecting the operator in the event of any catastrophic failures of the viewport, the “blast shield” reduces unwanted infrared fluctuations/reflections from external sources (on items such as the sample stage or the samples themselves) and prevents most accidental bumps or other movement of the camera setup.



*Figure 12 - Blast Shield, which sits around the camera and viewport*

## **2.4 Determining measurement point placement**

To obtain temperature data at certain points from the ResearchIR software, it was found that the most straightforward method was to place cursors on each point at the beginning of the test, gather the data at each point individually, then compile and analyze the data afterwards. Measurement points must be placed on the image in precise locations to obtain good data; as mentioned previously, the camera resolution giving enough pixels per millimeter to place the points with relative accuracy is important here.

Points must be set far enough apart to get good data which shows a clear difference in the temperature curves at the two points. Initially, the points on each side of the sample were set at 2mm and 6mm from the edge of the plane heater – totaling four points per sample (Figure 13). This corresponds with the locations of the four points measured in the previous method. However,



an additional point was added to each side of the sample during the development and trial of the new method, allowing the thermal diffusivity to be calculated three times per side (once between each possible pair of points, Figure 14) and the results compared to determine any sources of error and the relative accuracy of the method as dependent on point placement. The ability to add an extra two points on each side with little hassle is a major benefit of the infrared imaging-based method developed here, compared to the prior method which used thermocouples.

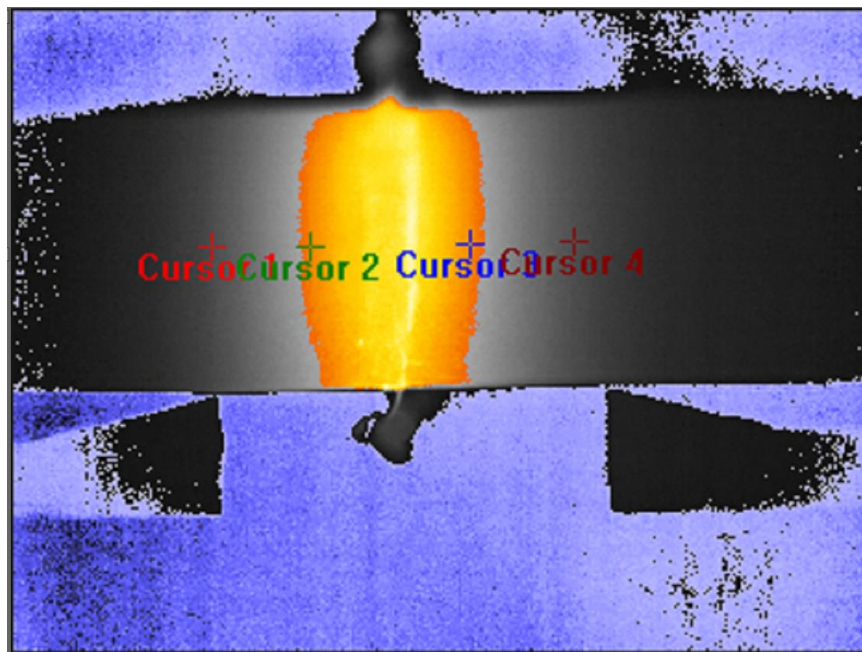


*Figure 13 - Four points set up for data collection (test F)*

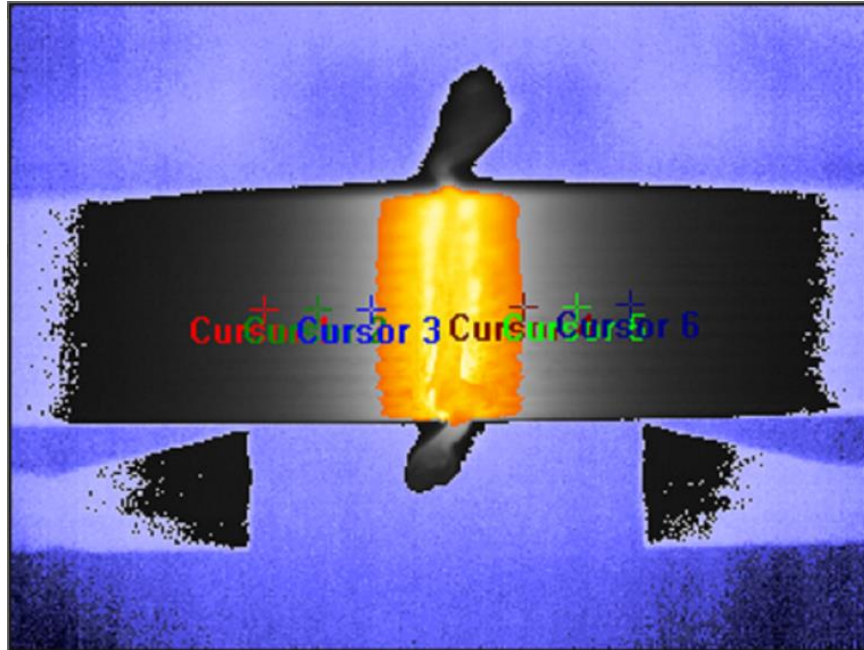


*Figure 14 - Six points set up for data collection (test K)*

Reference points are needed to determine correct scaling of the image in order to place the measurement points correctly. A solution to provide these reference points was one of the main driving factors in designing a new stage to hold samples. Once reference points exist within the camera feed, they can be used to determine the scale of the image and then place temperature measurement cursors on that image. A spreadsheet was created to simplify the process of measuring the camera input points and placing the cursors, and it will be covered in section 4.3.



### Chapter 3: Sample Stage Development

To hold the samples inside the vacuum chamber in place, perpendicular to the camera, a stage was designed and iterated upon. The initial stage (Figure 15) was made from pieces of acrylic sheet glued together to hold each sample out at the ends, away from the plane heater, and had rubber pads to hold the samples more securely. The final stage (Figure 16) holds the samples in place without issue and is simple to make using 3D printing, while ensuring that measurement points on the samples are placed correctly and reflections on the surfaces of the samples are reduced or prevented entirely.

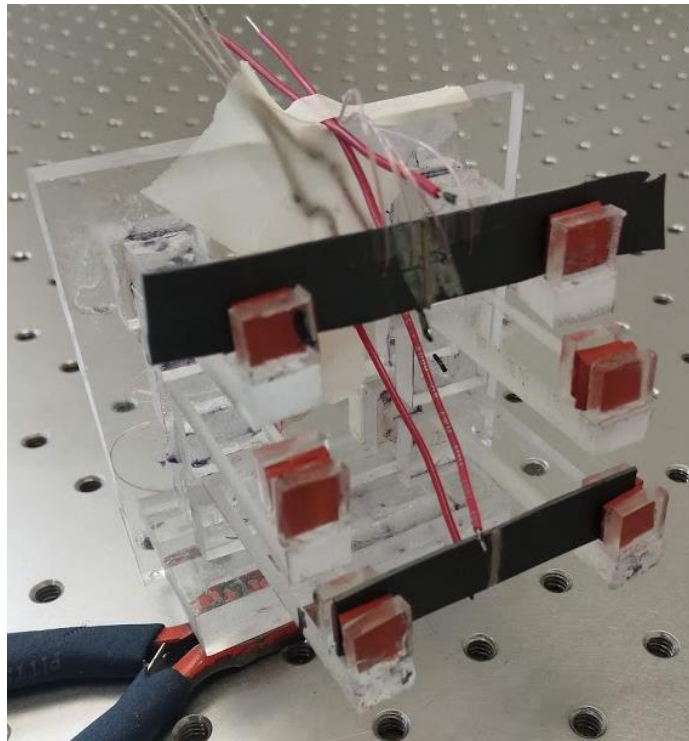


*Figure 15 - Initial sample stage design, made by Fatema*

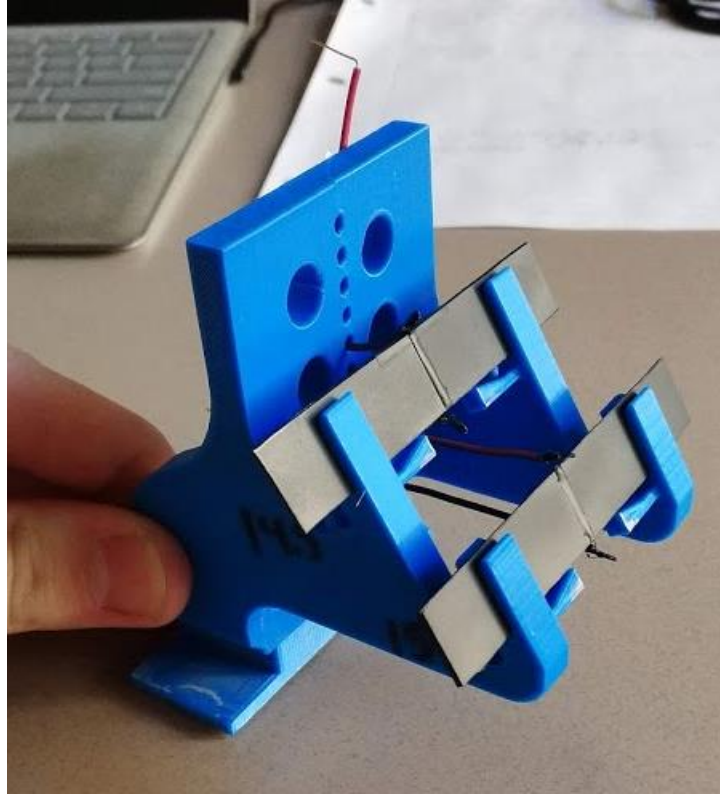


*Figure 16 - Final sample stage design MK3*

### **3.1 Reference datum**

To place the points (cursors) correctly on the camera feed within the ResearchIR software, the exact locations of the points in terms of pixels must be determined. However, to obtain the correct locations for the points, one must first know what distance a pixel width corresponds to on the physical sample. To determine what this scaling of pixels to millimeters should be, it was decided that two points would be placed on the sample stage at a fixed, known distance apart. These two points could then be located within the infrared camera feed and the distance between their coordinates, in pixels, converted to millimeters per pixel. This scaling process is integrated in the point placement spreadsheet which is covered in more detail in 4.3.

The reference datum points are integrated into the stage, using a design which is robust and easy to use. The reference points are on the end of protruding elements immediately below the sample. These elements are tapered linearly for two reasons: first, to keep contact with the sample to a minimum, providing only a single point at the tip of the element where it touches the sample (preventing most heat conduction into the sample stage); second, the element's outline is visually represented on the camera feed by two lines intersecting, making it easier to determine the exact coordinates of the point on its corner. The reference datum are shown in Figure 17.

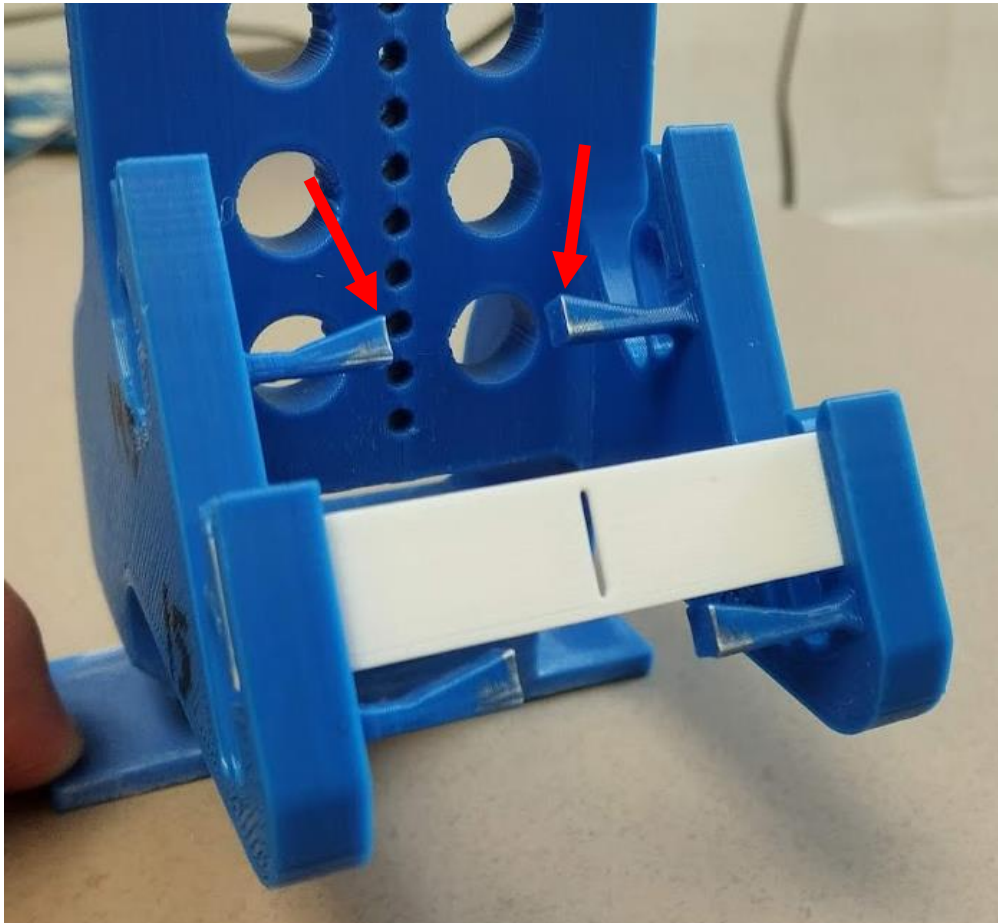


*Figure 17 - Reference datum on sample stage MK3*

### **3.2 Layback angle**

Prior research with an infrared camera, completed as part of the dissertation work of Dr. Christopher Dalton here at the University of Oklahoma, showed that when working with an infrared camera, there can be an issue with the camera picking up reflections of external heat sources off of an inspected planar surface [9]. This same issue was discovered during early experimentation with the system developed in this thesis—some samples were reflecting the heat of the infrared camera itself, causing the sample to “look hotter” to the camera in certain areas than it really was. To address this issue, taking inspiration from the redesigned shroud of Dr. Dalton’s work, samples were “laid back” at a 30° angle relative to the normal plane of the camera focus. This “layback” angle was designed into the sample-holding stage to hold the samples at a fixed, consistent angle. The samples are now angled such that any warm object held above the camera could be reflected into the camera by the samples, but this interference is prevented from accidentally happening by the “blast shield” discussed in section 2.3. Sample stage models designed with and without this integrated layback angle can be seen in Figure 18 and Figure 19.

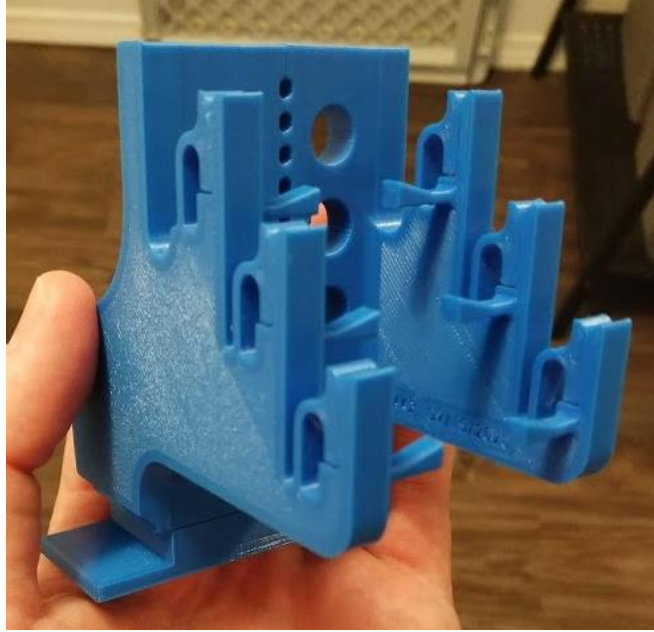


*Figure 18 - Sample Stage MK2, with no layback angle*

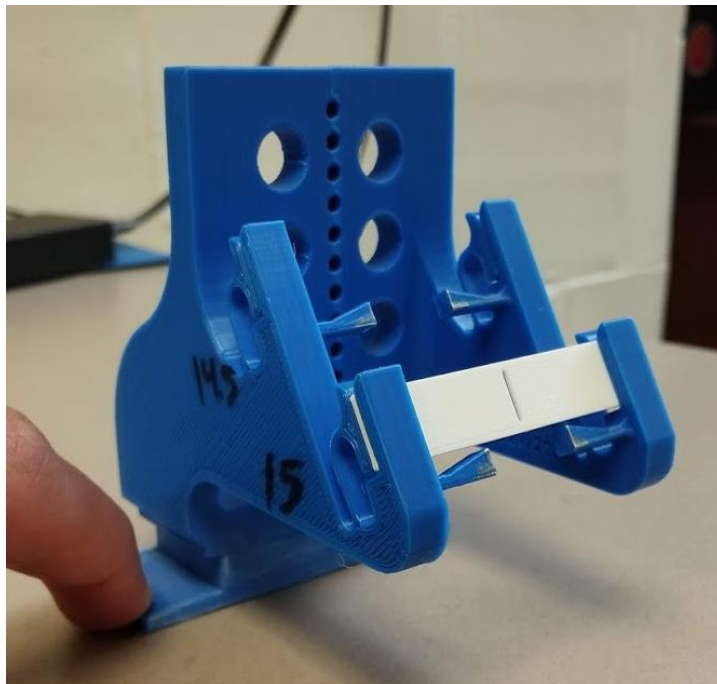


*Figure 19 - Sample Stage MK3, with 30° layback angle and PLA sample blank in place*

### **3.3 3D printing**

To manufacture the sample stage, the process of 3D printing was selected as the most effective method, and the sample stage was printed using PLA (polylactic acid) plastic filament. 3D printing the stage allowed for quick iteration of designs, complete interchangeability with prior versions of the sample stage, minimal effort required for assembly, and additional convenient design features (discussed in 3.3.2). However, designing for 3D printing required a few specific considerations.

#### ***3.3.1 Designing for 3D printing***

While 3D printing allows for creation of complex geometries with ease, it does require a special approach in designing the parts for them to print well on a standard FDM (fused deposition modeling) 3D printer. This style of 3D printer lays melted, extruded plastic, line by line on a flat surface known as a print bed, and sequentially higher layers of the print rely on the layers below to support them. If a design is made to be 3D printed, this requirement is often accounted for and overhangs are reduced as much as possible; if reducing overhangs is not possible or not done, extra “support material” must be added in lower layers to support those above, then broken away from the part once the print is complete. This wastes a small amount of material, but more importantly, it increases the print time and generally creates a rough surface on the finished part in the locations where the support material was broken off. In addition, detailed geometries and small parts are more difficult to print when support material is required for them. To prevent any of these issues, the part was designed to print in three sections flat on the print bed (Figure 20), then assembled into the final stage using simple slot-and-mortise and double dovetail joints with no glue required, and just snapped together. This design ensured the finished stage would be dimensionally accurate



with smooth surfaces and allowed for detailed parts such as the integrated sample clamps to be printed without issue.

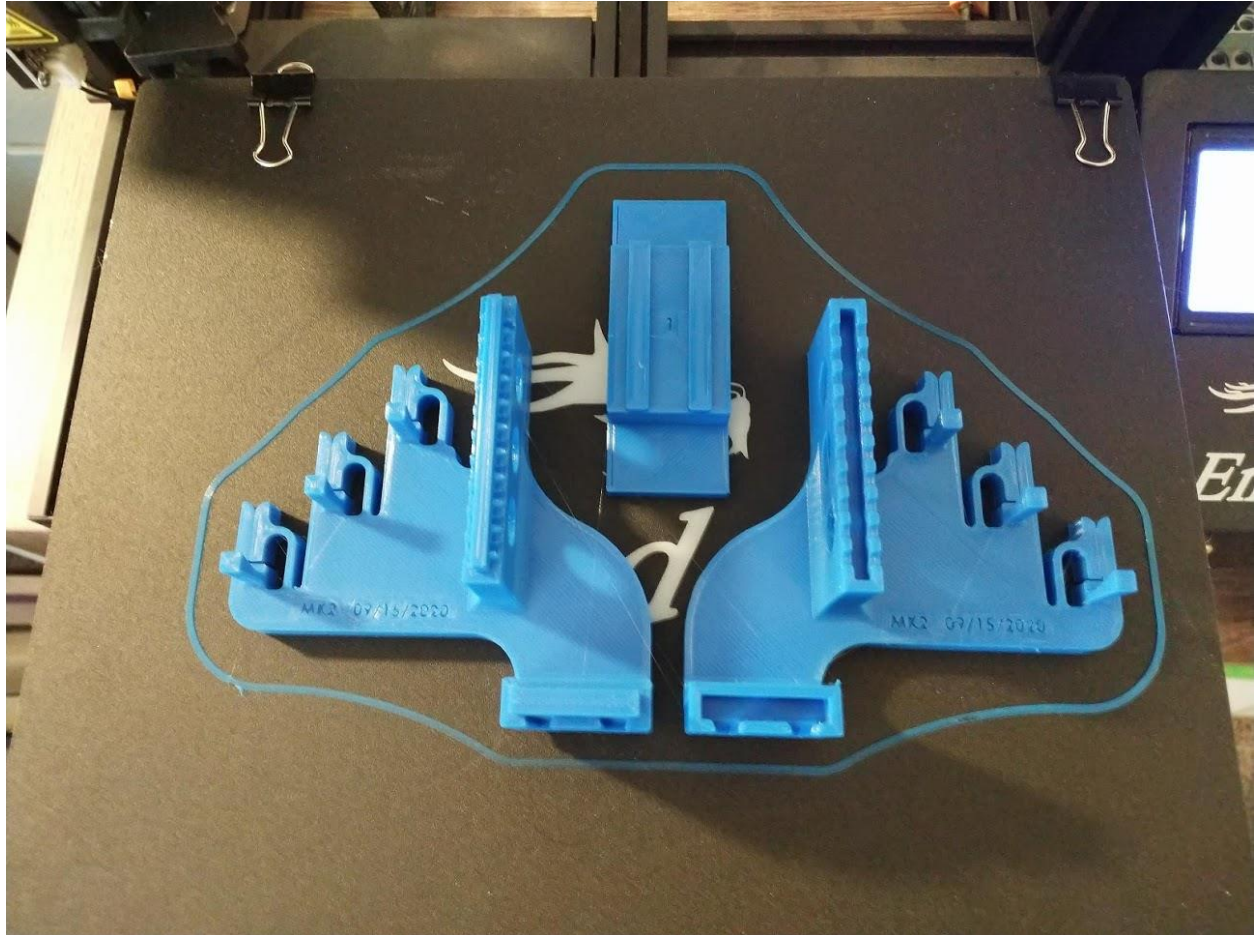


*Figure 20 - Print layout of Sample Stage (MK2 pictured)*

### ***3.3.2 Additional design features***

In addition to incorporating the previously mentioned design features of reference datum and a 30° layback angle, the final version of the sample stage was designed to hold the samples securely using integrated clamps. These integrated clamps are a simple compliant mechanism which consists of a front surface which the sample is pushed against, a clamp “head” which presses up

against the sample, and a thin piece of plastic which acts as a spring to provide a light amount of clamping force. These integrated clamps hold the samples in place from the ends of each sample, ensuring that heat is not conducted out of the inspection area directly into the clamps, which would skew the results. The main benefit of this integrated design is that no extra parts or materials are required to hold the sample in place. Simply print the stage design, assemble, and use immediately; there is no need to adhere rubber pads to the clamping surfaces or worry about the sample(s) falling out because the stage is too loose. The integrated clamps are seen below in Figure 21 and Figure 22.

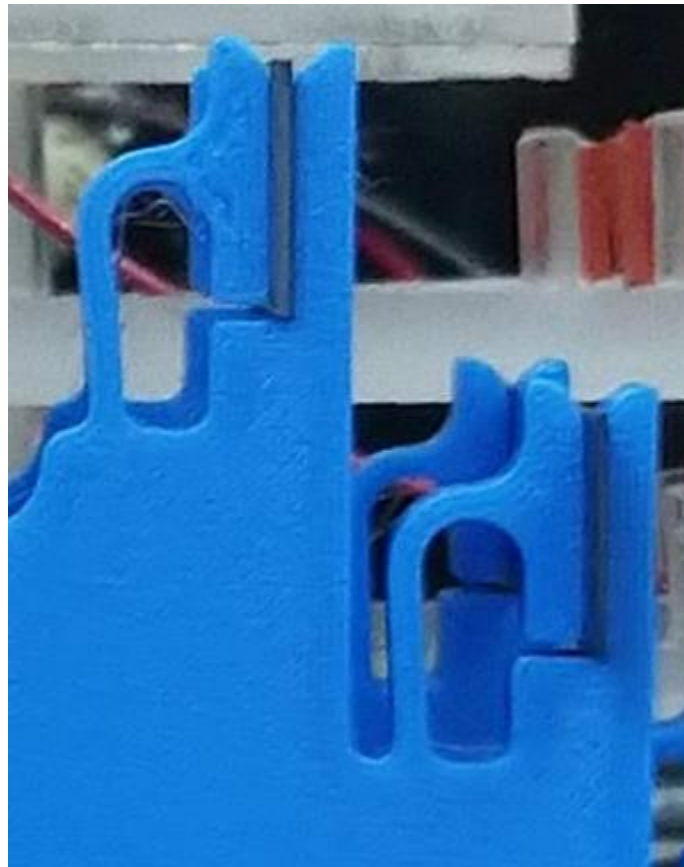


*Figure 21 - Integrated clamp closeup on MK2 model of sample stage, with samples in place*



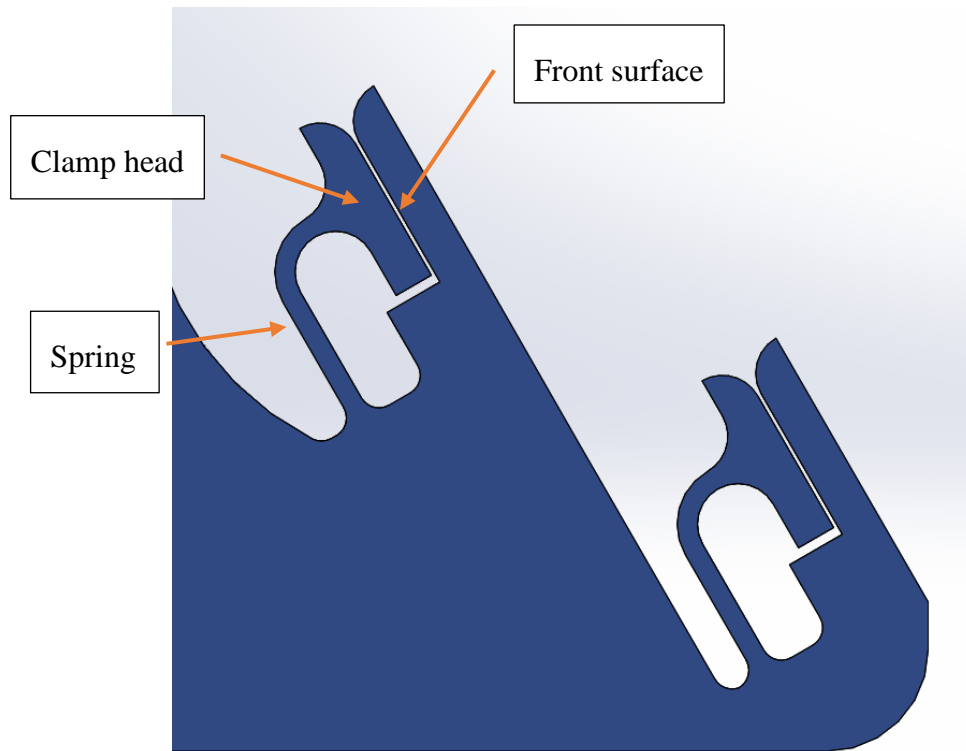


*Figure 22 - Integrated clamps of MK3 sample stage, side profile shown on SOLIDWORKS CAD model*

Two samples can be loaded on the stage, though only one at a time can be focused on by the camera and data gathered for it. While the data collection must be done one sample at a time, the vacuum chamber can stay pressurized between the two samples, saving time by not forcing depressurization between each test. Previous versions of the stage were able to hold three samples at once, but after redesigning with the samples angled back 30°, this was scaled down to only two samples for sample stage MK3.

The sample stage also has a perforated back, with many small holes down the middle to allow for wires to come off of the sample heater and through to the back of the stage, where they are taped in place. Fixing the wires in place in these holes reduces breakage of the fragile heater wire.

One other feature of the design is the method in which the sample stage is held in place within the vacuum chamber. The base of the chamber has an acrylic block adhered to it, and the top surface of that block has two acrylic tabs which create a channel for the stage to mount in. The stage is thus held in place and always positioned in the same spot when loaded into the chamber, making refocusing of the camera after reloading the chamber a snap. Figure 23 shows the sample stage loaded and ready to go in the vacuum chamber, mounted using this method.



*Figure 23 - Sample stage mounted inside vacuum chamber*

## **Chapter 4: Sample Measurement**

To gather data from the material samples examined, the system was calibrated to the modified surface emissivity, then samples were prepared (as detailed in section 2.1), placed in the vacuum chamber, had measurement points placed on the correct locations of the camera feed, and then were fed a sinusoidal heat wave over a long period of time. Once the test was completed, this data was gathered and analyzed for the examined sample.

### **4.1 Calibration of surface emissivity**

To ensure the camera is calibrated correctly to read the correct temperature at any given point, the camera must be adjusted to read the correct surface emissivity. Calibration of the camera was completed using an apparatus consisting of an aluminum plate, 1/8" thick and of dimensions approximately 20mm by 80mm, with applied heater and thermocouples. Aluminum was selected as the best material for this application because it has a high thermal conductivity and allows the calibration plate to hold a consistent temperature across the surface, as well as heat up quickly using the heater. First, shallow grooves were cut in the material to allow for more flush mounting of thermocouples within the front face of the plate. Two thermocouples were then adhered in those grooves using thermal epoxy and covered entirely with epoxy, and the epoxy was allowed to set. A resistive plane heater was then adhered to the back surface of the calibration plate to provide even heating across the entire plate (Figure 24). Once these steps had been completed, the same graphite spray used on the surface of the samples was sprayed on the front surface of the calibration plate to provide a thin, even coating of graphite (Figure 25).

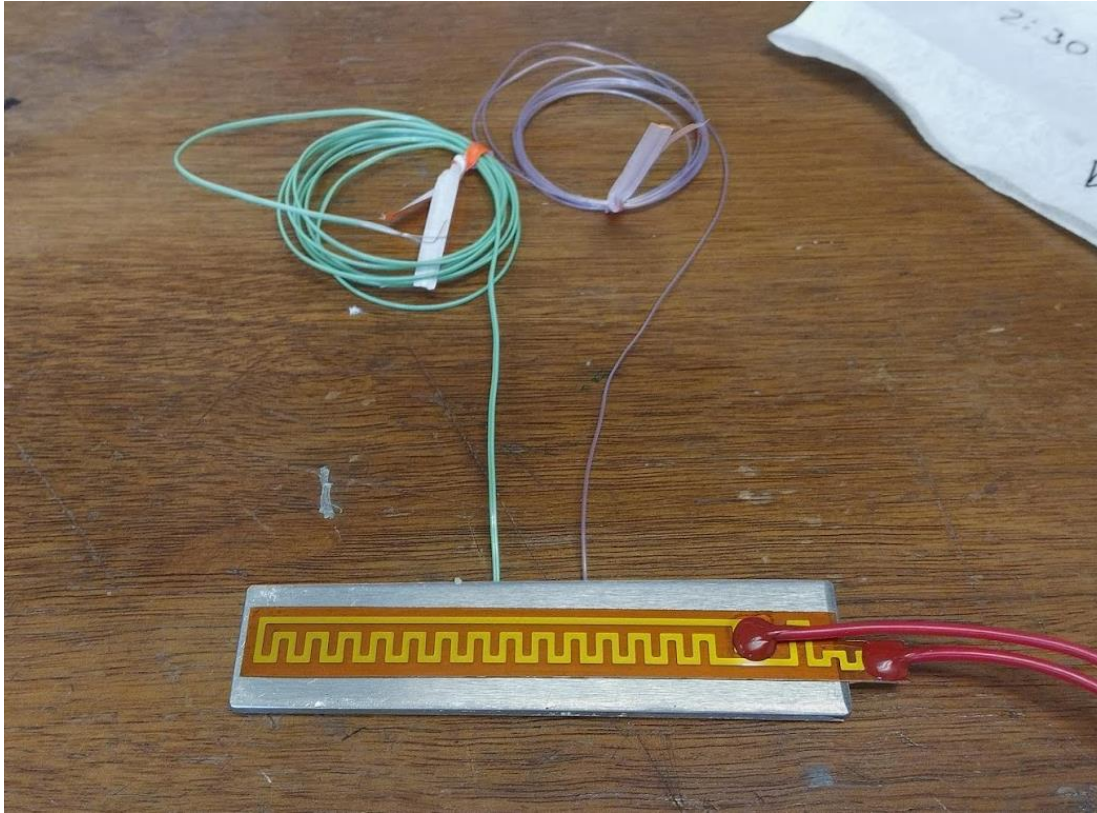


Figure 24 – Back side of calibration plate, with heater shown

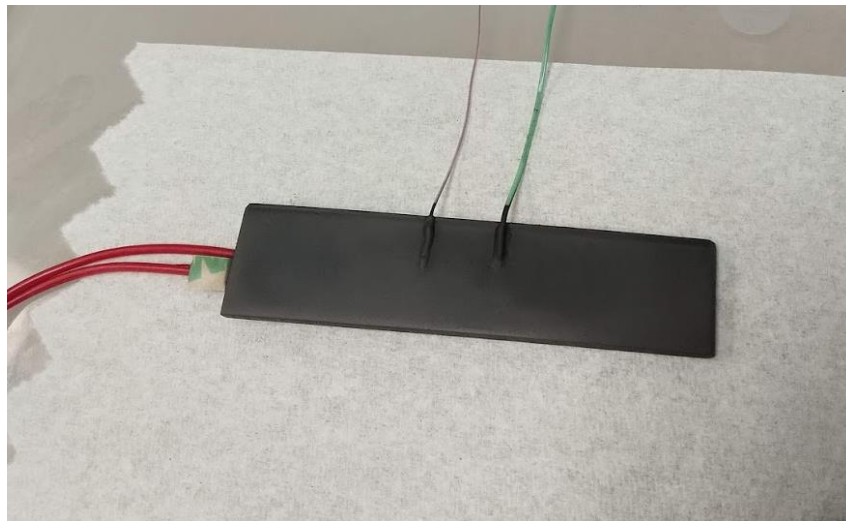
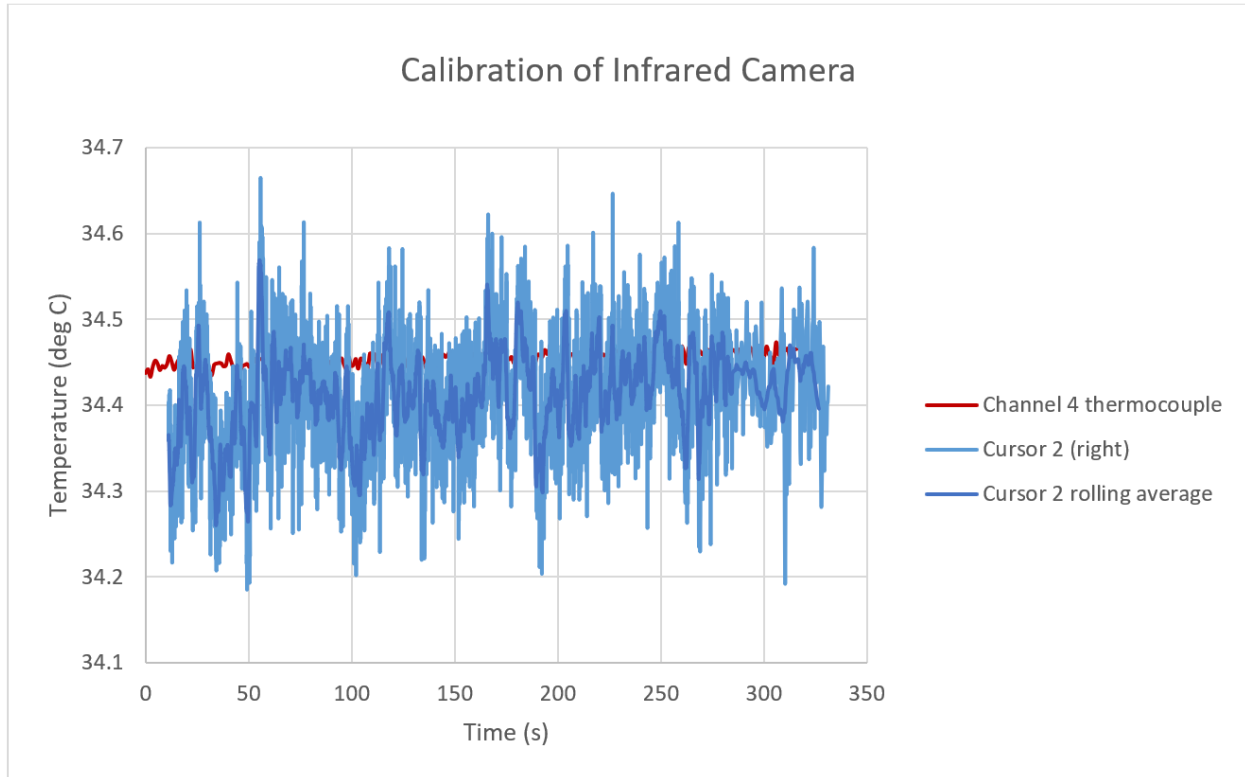


Figure 25 - Front side of calibration plate, with surface coating and thermocouple mounting shown

To calibrate the camera to match the surface emissivity of the graphite coating, the aluminum plate was placed in the vacuum chamber—on the 3D printed sample stage, tilted at the standard 30° angle—and heated at a low temperature using a constant voltage. Cursors in ResearchIR were placed on the thermocouple locations of the aluminum plate. The temperature of a thermocouple was then examined and compared to the temperature seen in ResearchIR.

A built-in surface emissivity calculator in the ResearchIR software took input of the actual temperature at a location, then gave the emissivity to be used at that location to get an accurate temperature output. This calculation was done a couple of times to be certain of the output, and the result was consistently that the surface emissivity coefficient should be 1.0. Emissivity of the image was set in ResearchIR to be 1.0, then data was gathered from both thermocouples and from two cursors set in their locations on the camera feed, for the purpose of verification.

This calibration verification resulted in data which showed the temperature of the thermocouples agreed fairly well with the infrared camera measured temperature after adjusting the emissivity. It can be noted that the camera data was very noisy in comparison to the thermocouple data. However, the amplitude of the noise is only about 0.2 °C. In the figure below (Figure 26), camera cursor data is displayed with a 16-frame rolling average overlaid, to cut out some of the noise.



*Figure 26 - Comparison of data from Calibration of Infrared Camera*

One can clearly see in Figure 26 that the average thermocouple values at each point were not perfectly aligned with the camera-gathered data. This could have been due to a few different factors, with one likely reason being surface variations due to epoxy lumped around the thermocouples, causing reflections of external heat sources to be included in the camera temperature measurement at those points. However, it was determined that this was a noisy but acceptable outcome, and the surface emissivity was found to be nearly 1.0 as expected.

#### **4.2 Steps completed for each measurement**

For each measurement of a sample, a series of steps were completed:

1. Turn on equipment, start ResearchIR software and ensure emissivity is set to 1.0
2. Load sample(s) in stage, then load stage into vacuum chamber
3. Seal chamber and pull vacuum
4. Run wires from sample's integrated heater to function generator, for heating of sample
5. Focus infrared camera on the sample to be examined
6. Place measurement cursors on the correct six points using a custom spreadsheet point locator (detailed in the next section) to place them at specific coordinates
7. Clear graphs for each point (sequentially) and turn on function generator
8. Allow the system to reach a state where the transient heat wave is no longer changing, while ensuring the maximum temperature seen in the material stays below glass transition temperature for the material
9. After a while where the transient state is not changing, save data at each point (sequentially)
10. Data collection is complete, move to next sample and repeat

### **4.3 Point locator spreadsheet**

To ensure accurate scaling of the infrared image and placement of the cursor points on that camera feed, a spreadsheet was built which takes input coordinates of several locations on the screen, then outputs the exact coordinates of where one should place the points. Coordinates of points A-J are found in ResearchIR by inspection of the camera feed, then input into the spreadsheet. The spreadsheet uses simple geometry to calculate the horizontal centerline of the sample, the points of intersection between that line and the edges of the plane heater, and the locations of each of the six points to place on the sample—along the centerline, appropriately offset from the heater edge. The two following diagrams give context for what this process looks like on the sample stage and

sample, as well as showing the camera frame boundary to signify approximately what is seen on the computer.

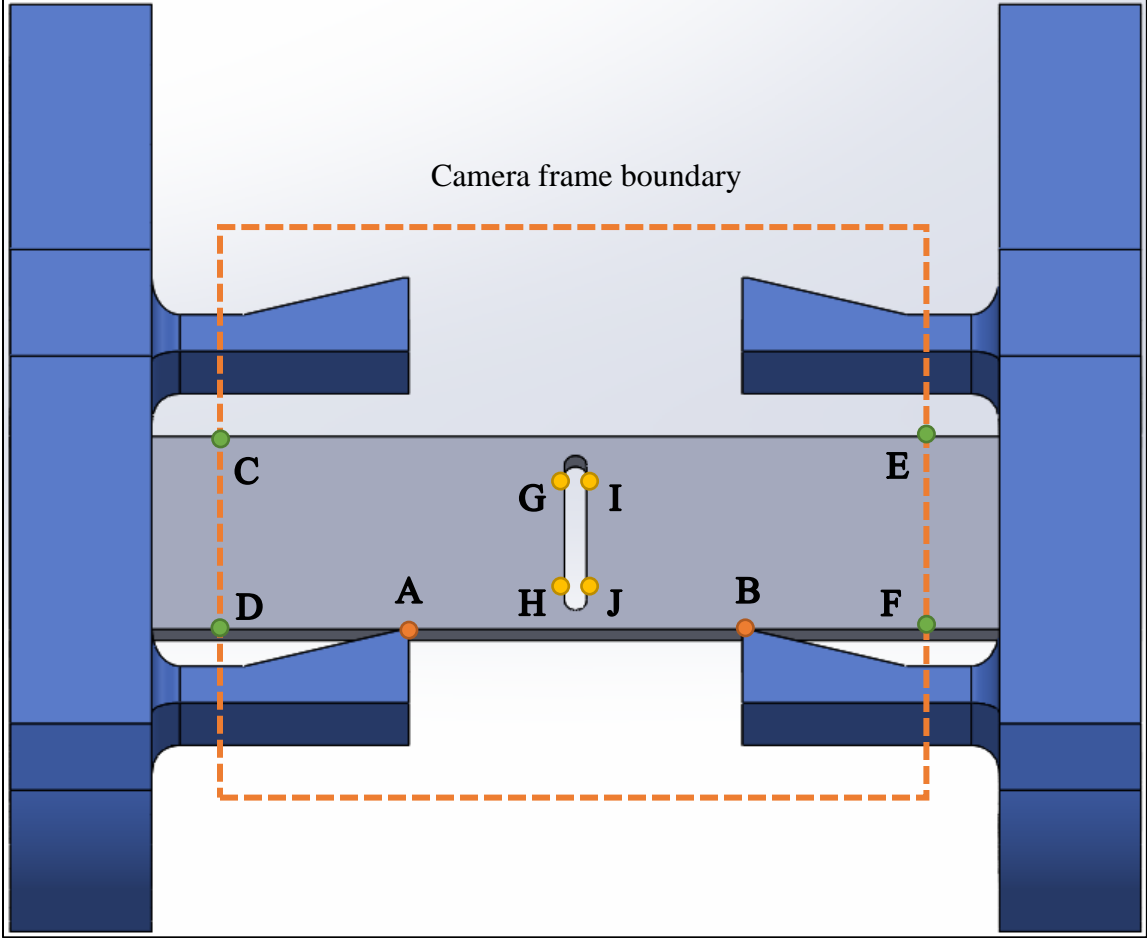
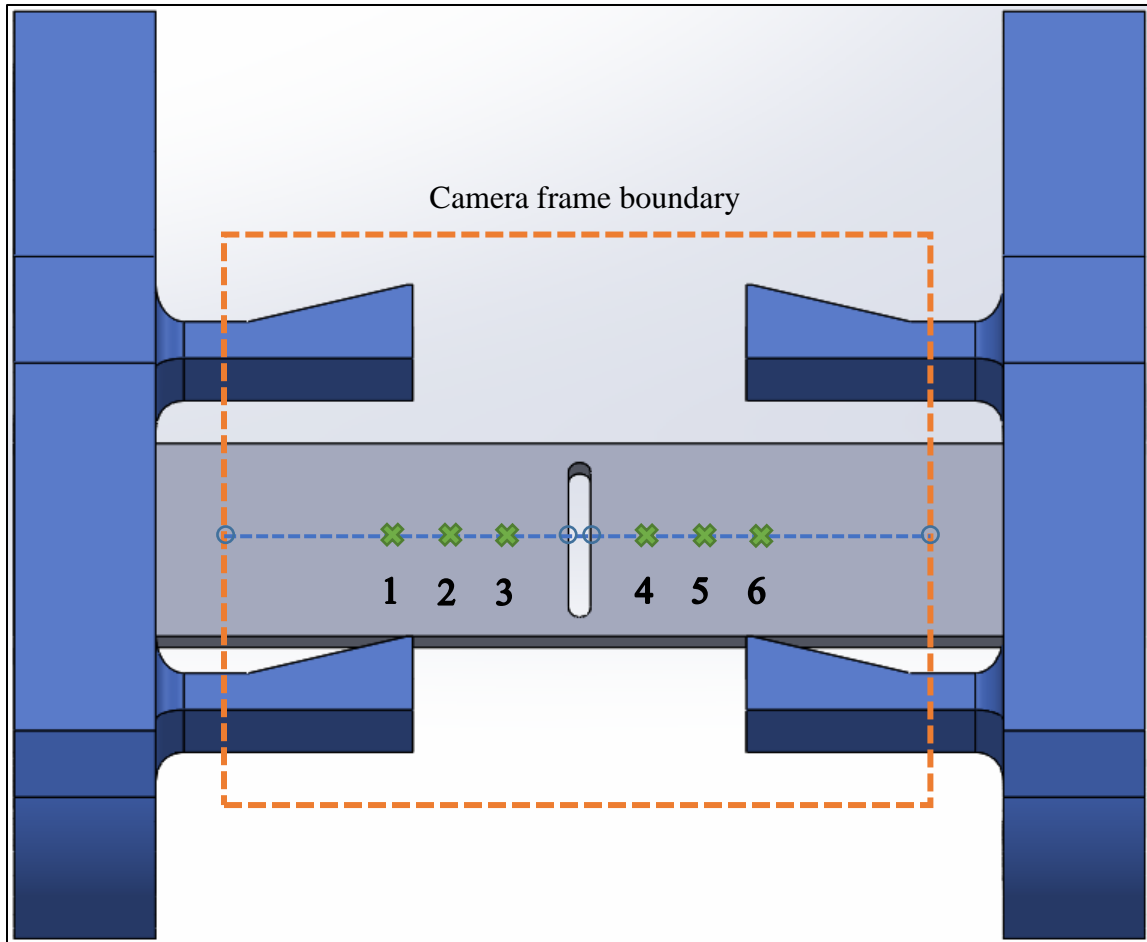


Figure 27 – Measured points, to take coordinates of in camera feed and input to spreadsheet





*Figure 28 - Cursor placement locations output, based on measured points*

In Figure 28, each of the four circles is a point which was calculated in an intermediate step. The process of finding a centerline for the sample is straightforward, as is finding the intersection of that centerline and the sides of the central heater. Once a centerline is constructed, placing points along that line is simply a process of using trigonometric functions to move along the centerline the correct distance for each point, starting at the intersection of the centerline and the edge of the heater. From this process, the points are all placed correctly on the sample, within the possible resolution.

## **Chapter 5: Data Analysis**

From the set cursor points / measurement points in the ResearchIR software, a plot of the raw temperature data at each individual point was obtained. Due to the method in which this data was gathered and the files were saved, the data sets first had to be aligned with one another. This was done simply using the video frame numbers to align each data set against the same relative time scale. Once the data was aligned, all six data sets could be visually inspected for obvious issues and to ensure the system had reached a state where the transient heat wave was not changing any longer. A representative plot of the combined data is pictured below in Figure 29, with a 5-frame rolling average used to smooth the data out a bit for visual inspection purposes. The data given as examples in this chapter is the output from an actual test (Test N) on a 3D printed PLA sample.

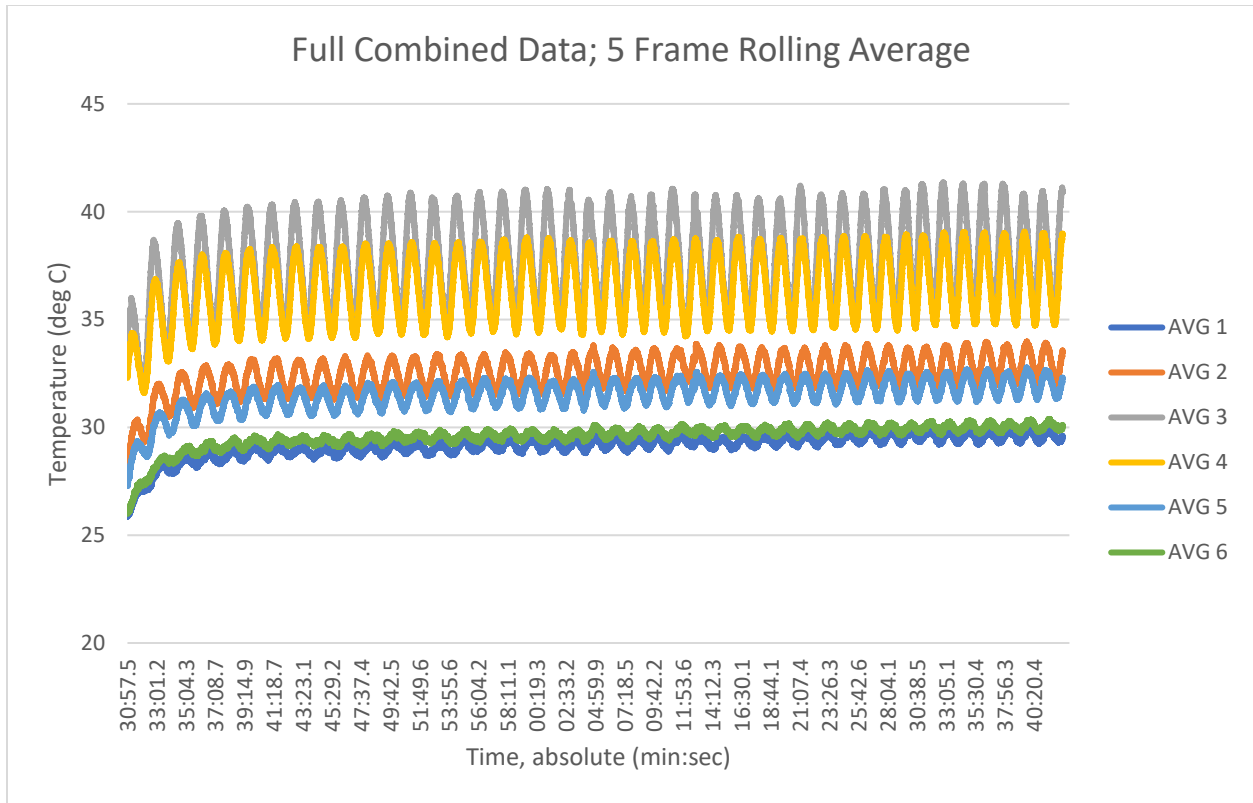


Figure 29 - Combined Data graph

One may note in this plot and those following that the data lines are labeled 1-6, corresponding to the measurement points set from left to right on the sample. It can be observed that there are some interesting discrepancies in the average temperature at each point, most notably that points 2 and 3 are significantly hotter than their counterparts 5 and 4 on the other side of the sample – this is likely due to the heating wire in the central plane heater being pushed to one side of the sample, or possibly having a better connection to the left side of the sample. However, the calculation of thermal diffusivity is based on the ratio of amplitudes between two points, the phase shift between them, and the physical distance between them, so the average temperature of one side being higher should not affect this calculation even if the two sides are not identical (see 1.3).

Once all the raw data is combined, a shorter representative section of the data is cut out for analysis. In this case, a section of 4000 frames is taken (starting approximately 6000 frames before the end of the test) and examined; taking a section well before the end of the data ensures that there is not any junk data included in the analysis which would throw off the curve fit. The narrow section pictured below in Figure 30 is just over 300 seconds of data, taken at the approximately 13 frames per second rate of data collection achieved by the camera in this test. At the 100 mHz frequency of applied voltage to the heater, we expect to see a peak temperature every 100 seconds and for this narrow section of approximately 300 seconds to show three full waves.

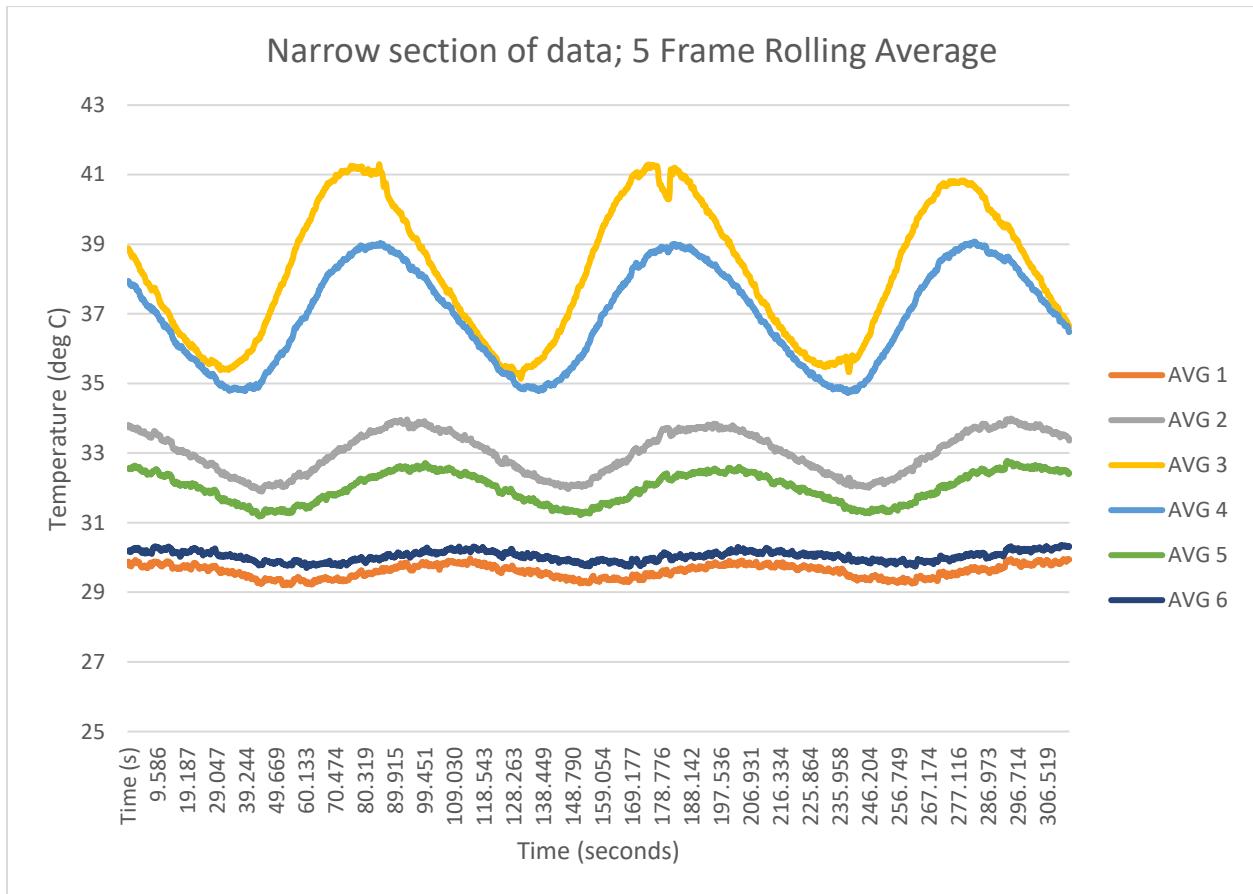


Figure 30 - Narrow Data graph

Once narrowed down, this data is inspected to ensure it matches what is expected based on the larger combined data graph. As mentioned above, the narrow section does indeed show three waves of heat, which is a good data set to fit a curve to – not so large that it overwhelms the solver, but large enough that it provides a good representation of the larger data set. It is worth mentioning again that the graph shown above shows a 5-frame rolling average for the sake of making the visual representation smoother, but the raw data is used for curve fitting and further numerical analysis.

## **5.1 Curve fitting**

Curve fitting for each of these waves, each representing the temperature at a given cursor, is completed with a spreadsheet built to use the Solver add-in within Microsoft Excel. The spreadsheet used was originally constructed by Dr. Jivtesh Garg for application with the prior measurement method, then adapted slightly for use in this new application. First, an approximation for the curve is created using a sinusoidal model. The sinusoidal model approximates the temperature curve with three components: an initial offset which is set to roughly the average temperature, a primary sinusoidal component which closely matches the actual curve, and a higher order harmonic of low amplitude which often just deforms the sine wave a bit to better match the actual data. These three components are dependent on five variables: one for offset, then an amplitude and a phase variable for each sine wave. The least squares method was used to get a single value which the Solver add-in then works to minimize: a measurement is gained of the error between the actual data and the approximation at each frame's time, then the square root of the sum of the squares of each individual error is taken as the single value to minimize. As the Solver works to minimize this error, the approximation approaches a close match to the actual data. Generally, for data which shows a clean sinusoidal wave to begin with, the approximation looks quite good. Approximations for three cursors are shown below as an example.

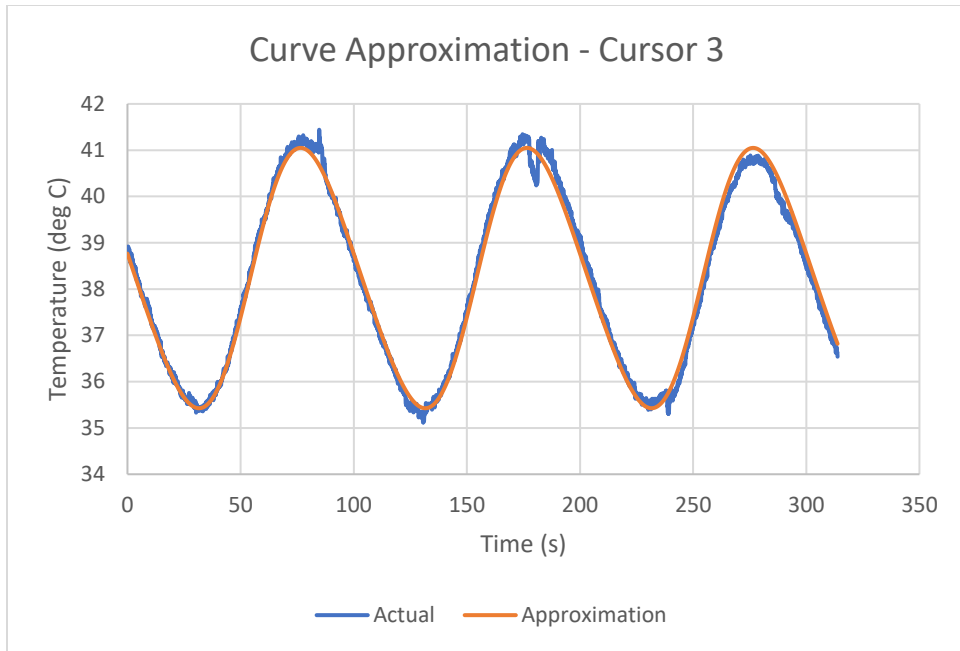


Figure 31 - Curve approximation - Cursor 3

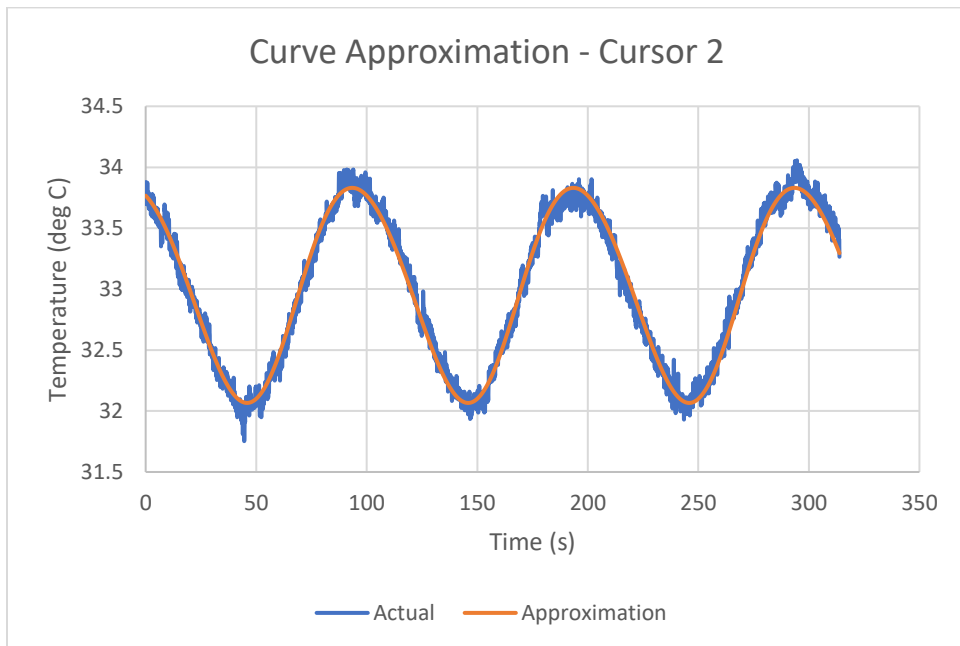
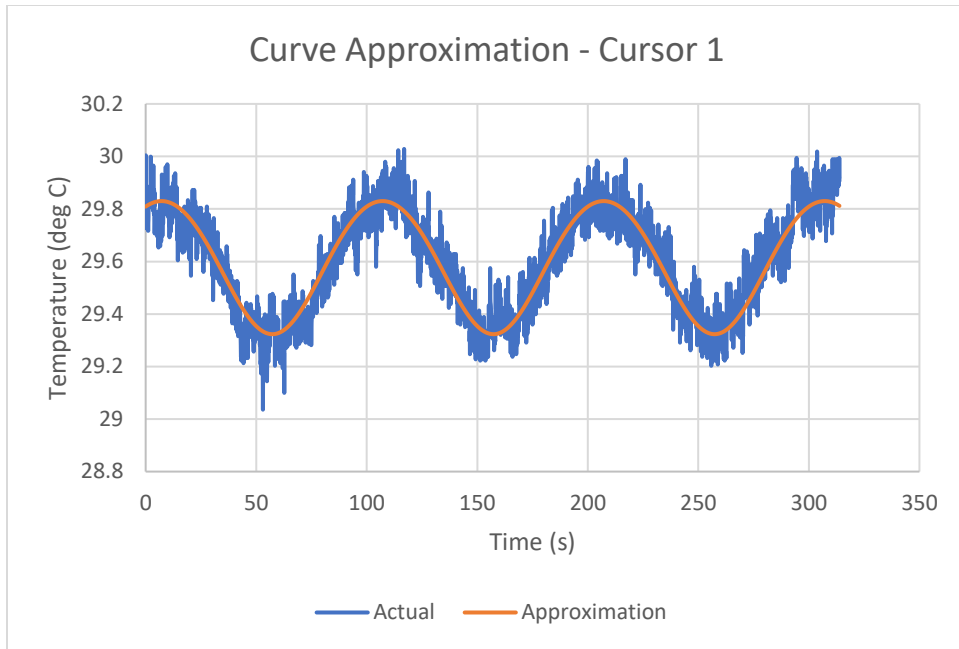


Figure 32 - Curve approximation - Cursor 2



*Figure 33 - Curve approximation - Cursor 1*

The left side of the sample is examined in these three curve approximations, with each cursor receiving its own graph of the raw data and its approximation. Each approximation fits the data well, but the increase in noise as the points are further away from the heater (with Cursor 1 being the furthest of the three from the heater here) becomes obvious. This phenomenon will be discussed in more detail later with discussion of results.

Once each approximation has been solved for and refined to an acceptable degree, final approximations are plotted together (Figure 34) for comparison to the narrow data plot (Figure 30). (Note that the colors may not be the same between the two plots.)

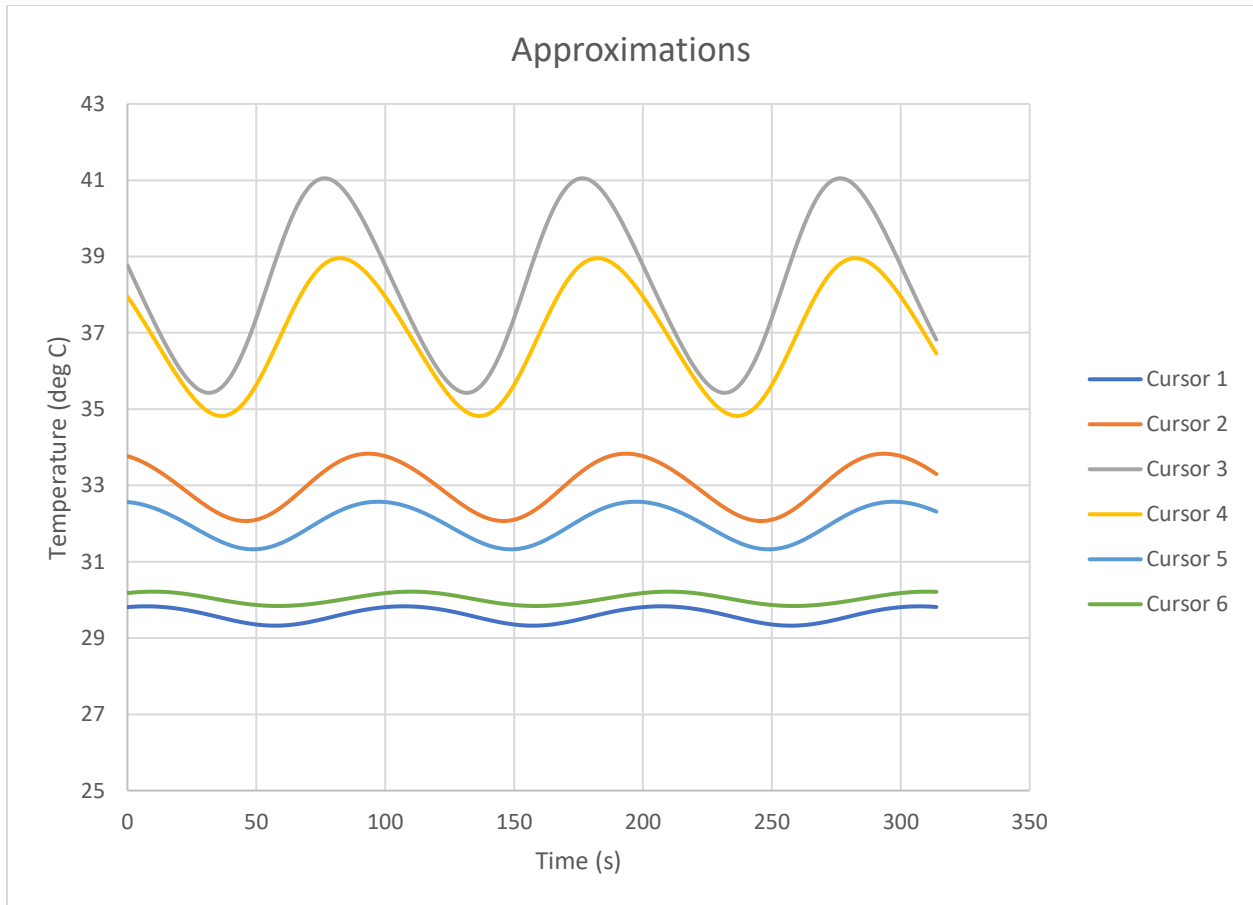


Figure 34 - Combined Approximations

To obtain thermal conductivity, one must first obtain thermal diffusivity. As per the explanation of Angstrom method, the thermal diffusivity is calculated by taking two sinusoidal heat waves, at two points along the sample, and calculating both the ratio of the amplitudes of the heat waves and the phase shift between the two. Conveniently, values have already been calculated for the phase and amplitude of the main component of each sinusoidal approximation. With these values, Equation 1 can be used to easily calculate the thermal diffusivity between those two points. Once thermal diffusivity is obtained, material properties of density and specific heat can be used to convert this thermal diffusivity value to thermal conductivity, where this is desired.



## 5.2 Automation of Analysis

To improve and simplify the analysis technique, software-based process automation techniques were implemented. By automating much of the analysis process using programs, human error in the analysis process is virtually eliminated. This compares to the prior method which relied on manually selecting and copy-pasting of many large chunks of data for curve fitting, then manually assembling the results of each curve fit to obtain a result. Automating this process also gives a massive reduction in data analysis time since it effectively turns the whole analysis into a one-step process with manual verification at the end, and provides many more chances to catch errors since visual representations of the data are automatically given at each step along the way. Finally, automating the analysis process allows for an easy increase in the number of data points analyzed without increasing human workload by any significant amount, allowing for further verification of data.

Macros/programs were coded in Visual Basic for Applications in Microsoft Excel to automatically complete analysis of the data. Microsoft Excel was selected as the best program for this data analysis because the prior method used an Excel spreadsheet for data analysis, and it was determined this method would be the easiest and friendliest for future researchers to adapt to when using this method to determine in-plane thermal conductivity of materials. Program code is present in the Appendix of this document.

## **Chapter 6: Results**

### **6.1 Data obtained**

Thermal diffusivity is presented here for all data points rather than thermal conductivity, since it is only dependent on the data gathered and is not dependent on other material properties such as density and specific heat. Measuring those material properties is straightforward but was not necessary for the purpose of validating this measurement method.

#### ***6.1.1 Polypropylene***

Two polypropylene (neat) samples were made, and several tests done on these samples for the purpose of comparing the accuracy of the method to other methods. While several tests were completed on polypropylene, the various tests changed a little bit over time as the method was refined. Results of calculated thermal diffusivity obtained from these tests are presented below, followed by some discussion of the results.

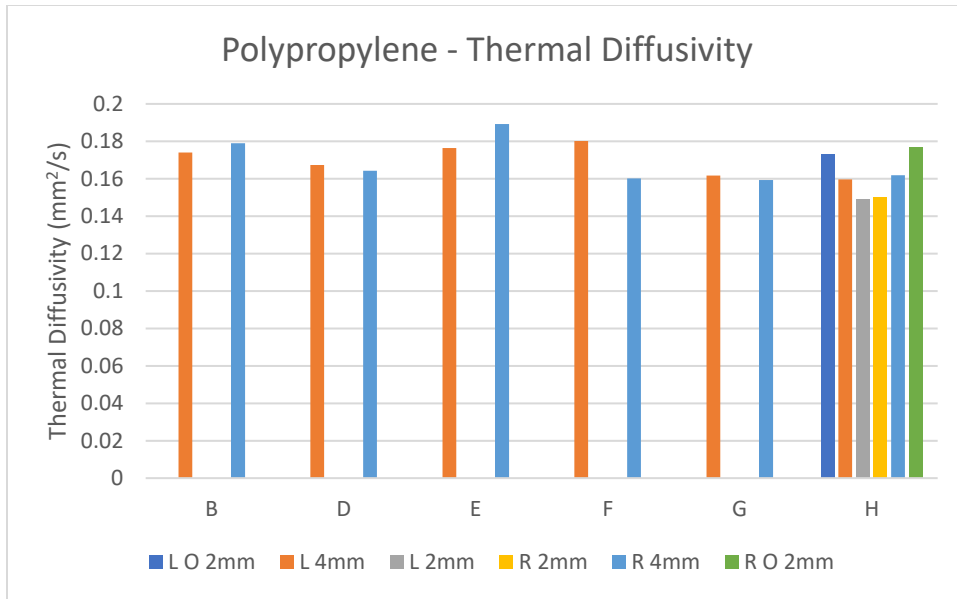


Figure 35 - Thermal Diffusivity of Polypropylene

In Figure 35 and following similar charts of results, up to six thermal diffusivity calculations are made per sample – three calculations made on each side of the sample using the three points placed on that side. The legend for these calculations is explained as follows (using point numbers as shown in Figure 28):

- L O 2mm is left side, outermost 2mm spacing (between points 1 and 2)
- L 4mm is left side, 4mm spacing between points examined (between points 1 and 3)
- L 2mm is left side, innermost 2mm spacing (between points 2 and 3)
- R 2mm is right side, innermost 2mm spacing (between points 4 and 5)
- R 4mm is right side, 4mm spacing between points examined (between points 4 and 6)
- R O 2mm is right side, outermost 2mm spacing (between points 5 and 6)

In an ideal situation, these six calculations would produce exactly the same result. However, due to various sources of error, the results often vary based on the calculation points. These sources of error are discussed further in 6.3.

Note that for tests B – G, each test result is presented as only two calculated diffusivity values. This is because these tests were completed with only four measurement points placed on each sample and thus only two diffusivity values can be calculated – one for each side – corresponding to the L 4mm and R 4mm labels. Test H was completed with ten measurement points, but only six values were calculated from this, using the six points closest to the central heater (three points on each side). The other four data points in test H were not used, because they resulted in data which had an amplitude too low in comparison to the noise to be approximated properly. Tests B, D, and E all had acceptable data obtained and were able to be analyzed; however, these three tests were early on in the process and upon further examination of the results, the system was not powered on for long enough to allow the transient state to stop changing in each test. For this reason, these test results are not being considered in the average value calculated.

Taking these exclusions out, and averaging the values of test H separately so they do not hold more weight than the other results, the average thermal diffusivity of the polypropylene samples, as determined through experimentation, is  $0.164 \text{ mm}^2/\text{s}$ .

### ***6.1.2 Expanding to other materials***

In addition to polypropylene, a couple other types of samples were tested using this method, providing further insights into the method and its suitability for different types of materials. As discovered in Test H, six cursors (three on each side, spaced every 2 mm from the edge of the

heater) was a good number of cursors to give enough data to examine without adding poor quality data. After this determination, six cursor points were used in every test.

### ***6.1.3 Polylactic Acid***

The next material examined was PLA, or polylactic acid, a thermoplastic which has grown in popularity and usage in recent years [10], [11]. The samples examined began life as a roll of white Hatchbox brand PLA 3D printer filament and were printed in such a way as to give each one an aligned layer direction. This was accomplished by changing slicer settings to generate GCODE for the printer which printed two samples with each inner line aligned at a 45° angle to the longitudinal direction of the sample, two samples aligned at a 90° angle, and two samples at a 0° angle. A screenshot of the slicer is provided in Figure 36 for illustration of the different angles to which the layer lines were set relative to each sample.

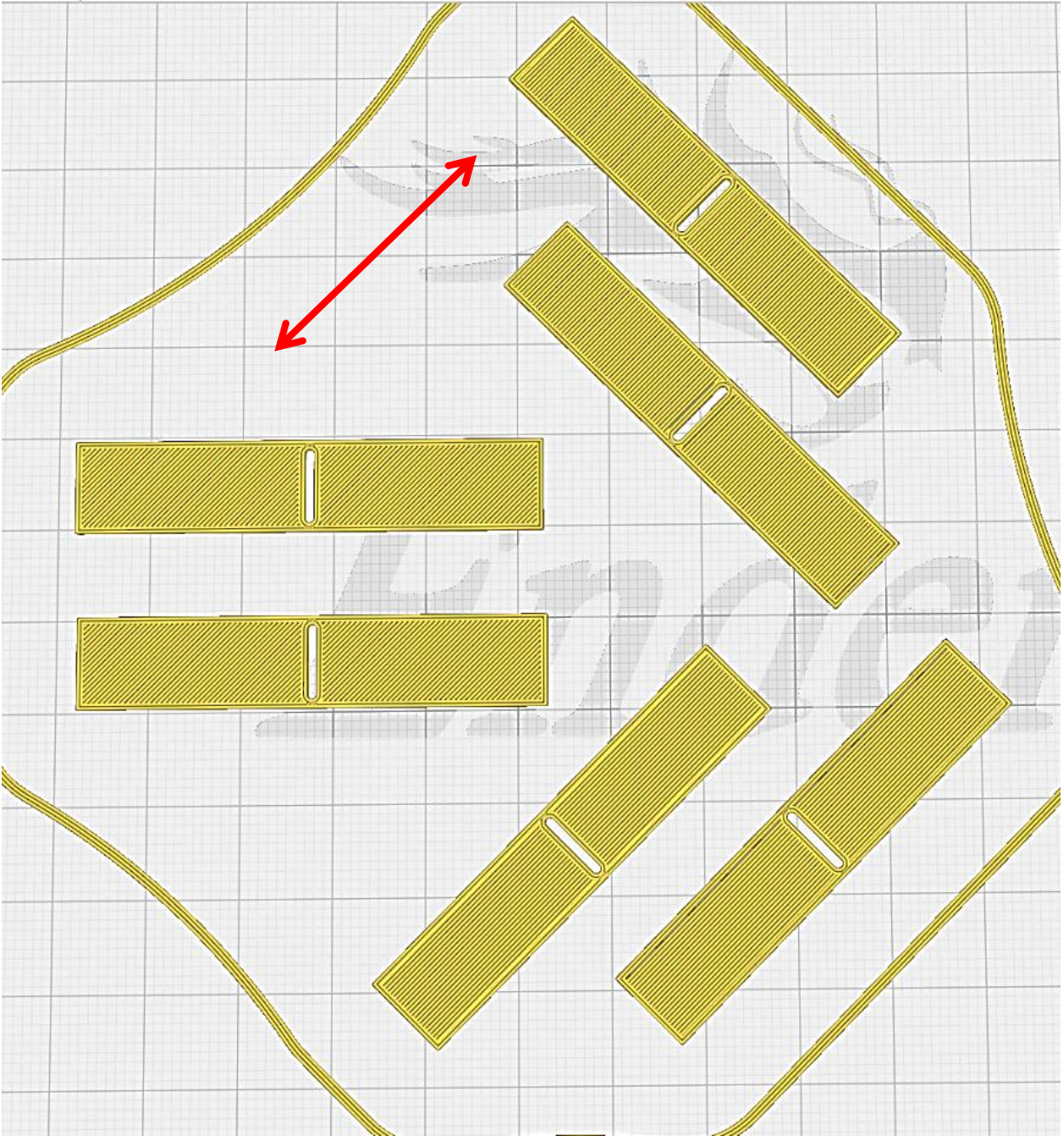


*Figure 36 - PLA samples pictured in Cura slicer software, with the red arrow demonstrating direction of alignment in layers*

This produced samples with three different angles of alignment between the layer lines and the direction of heat conduction through the sample (from the central heater outward). This was done

partly to examine the effects, if any, of the layer line print directions on the heat transfer through a solid 3D printed part. However, it also served as an interesting experiment to learn more lessons about the shortcomings of the infrared camera-based thermal diffusivity measurement method.

Data was gathered from tests on six PLA samples, with two samples tested of each directional alignment. The results are seen in the chart below, Figure 37.

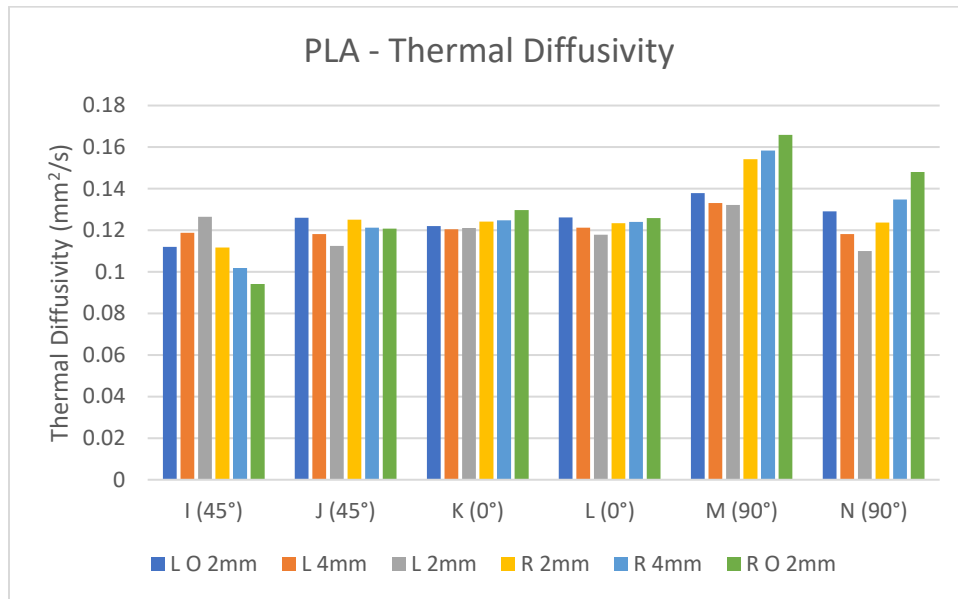
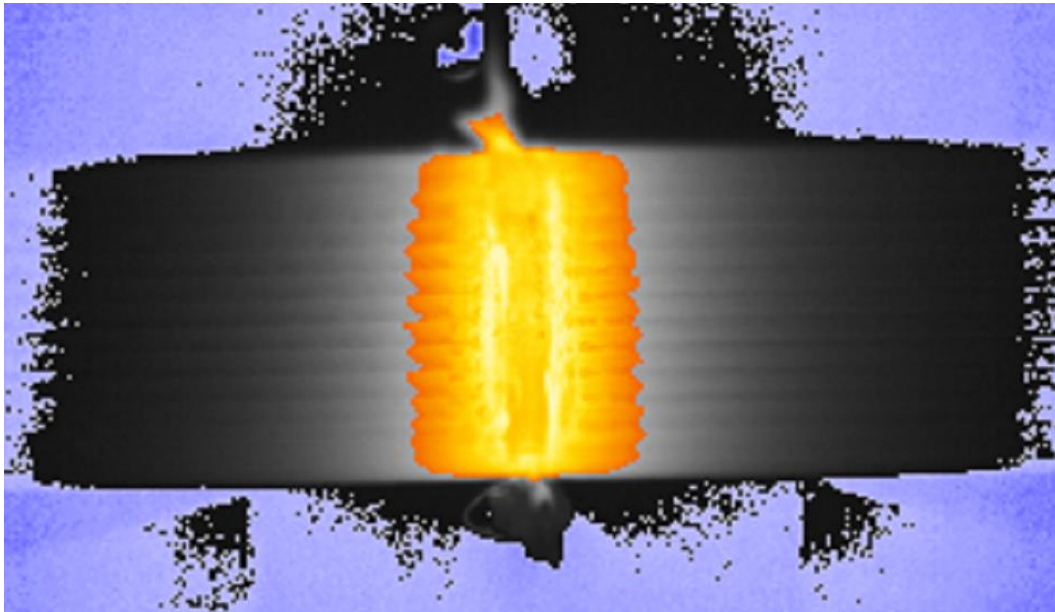


Figure 37 - Thermal diffusivity of PLA 3D printed samples at different layer angles

The results obtained from the PLA tests are all similar, though the 0° samples (tests K and L) had much more consistent results, with less variation. It appears there is not a significant difference in thermal diffusivity due to alignment of the polymer and layers in printing, and the average thermal diffusivity of all six samples/tests (36 calculations in total) was calculated to be 0.125 mm²/s. However, a more important take away from this set of tests is that the surface of the sample is very important to the error seen in the diffusivity calculations. This take away can be gained by

examining images of the samples during the tests, specifically taking note of where the temperature cursors are placed and what the temperature variation across the surface of the sample underneath looks like. First to be examined is one of the 0° samples, in the following figures.



*Figure 38 - Temperature variations on surface of 0° (longitudinal) PLA sample (test L)*



*Figure 39 - Cursors placed over variable temperature surface (Test L)*



Examining these images, the surface of the sample is not at a consistent temperature, and that the ridges produced on the surface by 3D printing the sample are slightly warmer than the surrounding valleys. The cursors were placed along a ridge on one side and along a valley on the other, but this is not important; what is important is that the cursors are not placed differently from each other on a given side. This caused the heat imbalance due to the surface texture to affect each point equally and produce very good results with little variation, and the surface variations were not an issue for these tests.

By contrast, examining the point placement from the 90° and 45° samples shows that there is some variation in the point placement on the surface of the sample – some points were placed on “hotter” parts of the surface (ridges) and this likely caused some of the variation in results. These samples are shown in the following two figures.

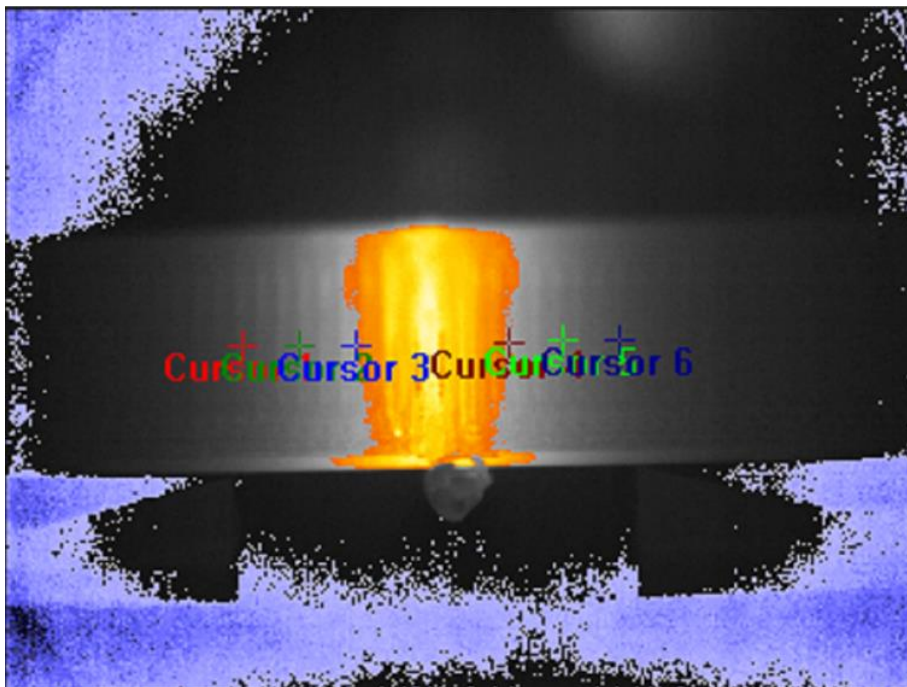


*Figure 40 - Cursor placement over variable temperature surface of 90° sample (test M)*

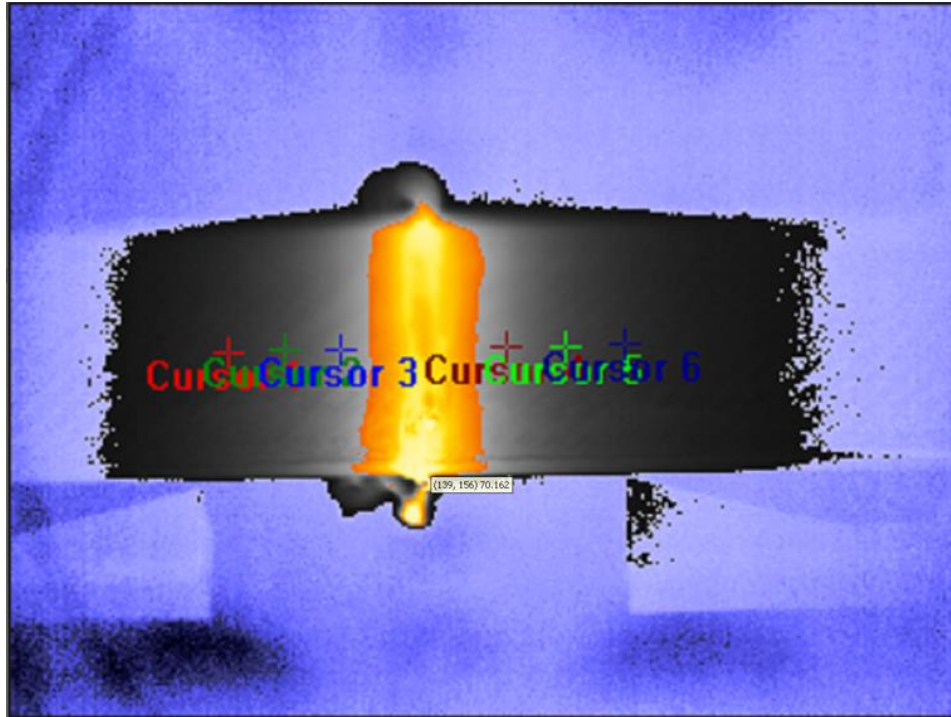


*Figure 41 - Cursor placement over variable temperature surface of 45° sample (test I)*

It can be seen in Figure 40 and Figure 41 that the cursors are not consistently placed on either a “peak” or a “valley” of the surface, but rather they are placed on either one at random. This causes some variation in the temperature curve at those points, reducing stability and accuracy of the final calculations.

#### ***6.1.4 Graphene-thermoplastic nanocomposite***

A graphene-thermoplastic material was created using solvent casting by Swapneel Danayat, another researcher in our lab, and a portion of this nanocomposite sheet was offered as a material from which experimental samples could be made for testing of this new in-plane thermal

diffusivity method. The thermoplastic used in this application was polyetherimide, and solvent casting was selected in part because of the high melting temperature of polyetherimide—which made other methods of mixing the particles into the base polymer difficult. However, it should be noted that the material used to make samples from had visually apparent defects and the graphene nanoparticles present within were not dispersed evenly through the material. These defects can be seen in the image below, where the thin samples were held up to sunlight and translucent spots showed up where the light came through.



*Figure 42 - Graphene/polymer nanocomposite samples, defects showing*



*Figure 43 - Graphene/polymer nanocomposite samples, same as above but overexposed to show the extent of the defects.*

In spite of the defects, samples were created and tested to see what would happen. Results from the testing of two different samples, cut from the same sheet of material, are below in Figure 44.

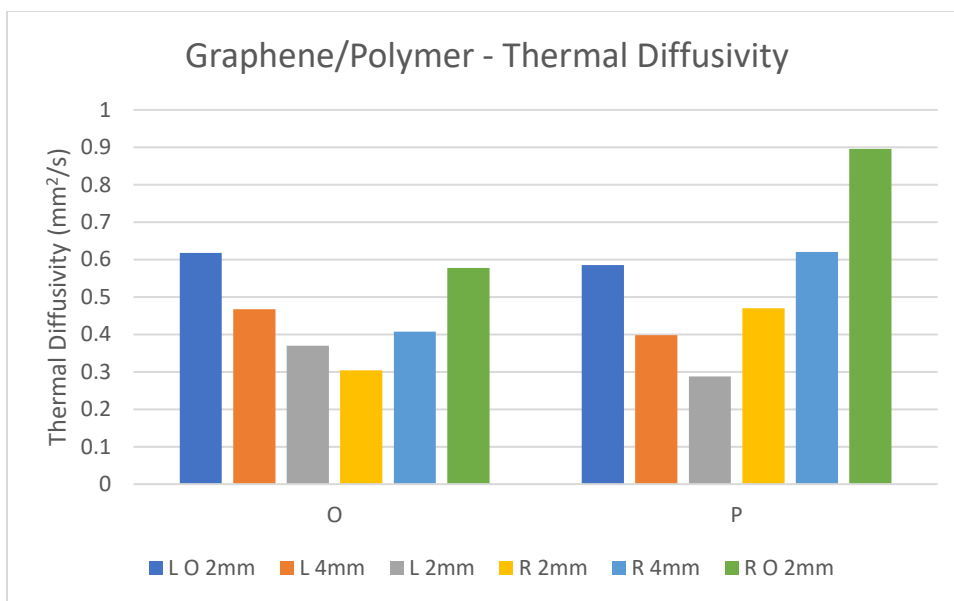


Figure 44 – Thermal Diffusivity of Graphene/Polymer nanocomposite

Taking the results at face value, the graphene-thermoplastic material examined does not have a clear in-plane thermal diffusivity value. However, context of the samples should be examined to determine what useful information can be learned from this data. Test P was completed on the bottom sample pictured in Figure 42 and Figure 43, which has apparent defects on both sides, indicating a very inconsistent graphene particle concentration. The presence of these defects likely explains the wild variation in the thermal diffusivity calculations for test P. Test O was completed on the top sample pictured in Figure 42 and Figure 43, which still contains defects, but contains far fewer of them. If it is assumed that the points closer to the heater will be more accurate (reasoning for this to be discussed in section 6.3), taking the average of the two innermost values calculated, it is determined that the thermal diffusivity of the sample used in Test O is somewhere around an average value of 0.34 mm<sup>2</sup>/s. This data is not particularly useful since it has such strong

inaccuracies, but it was an interesting trial of a thinner-than-usual sample which showed the effects of bad defects in the material.

## **6.2 Agreement with published values, other methods**

To validate the data gathered, thermal diffusivity values obtained from the experimental method were compared to thermal diffusivity values obtained through different methods.

### **6.2.1 Polypropylene samples**

Published values for the thermal properties of polypropylene vary based on what specific blend of polymers is present (block copolymer, random copolymer, or homopolymer), and the exact composition of the sample material used is not known (though it is suspected to be random copolymer) [12]. This is complicated by the fact that many published values do not list the type of polymers used; however, some high-quality published values can be found [13]–[15]. It is also true that when comparing thermal diffusivity values, one must note the temperature at which the diffusivity was measured [16]. In polymers such as polypropylene, thermal diffusivity varied greatly based on temperature in tests completed by Zhang and Fujii – in general, it was higher at lower temperatures for polypropylene [14].

Using the experimental setup,  $0.164 \text{ mm}^2/\text{s}$  is what was found as an average value for thermal diffusivity of the polypropylene samples. This thermal diffusivity was measured at a fairly low temperature, around  $33^\circ \text{ C}$  on average. Using the data for polypropylene random copolymer thermal diffusivity versus temperature from Zhang and Fujii, a linear curve fit was assigned to the first six data points and used to extrapolate what the thermal diffusivity would be at  $33^\circ \text{ C}$  [14]. The data is shown below in Figure 45.

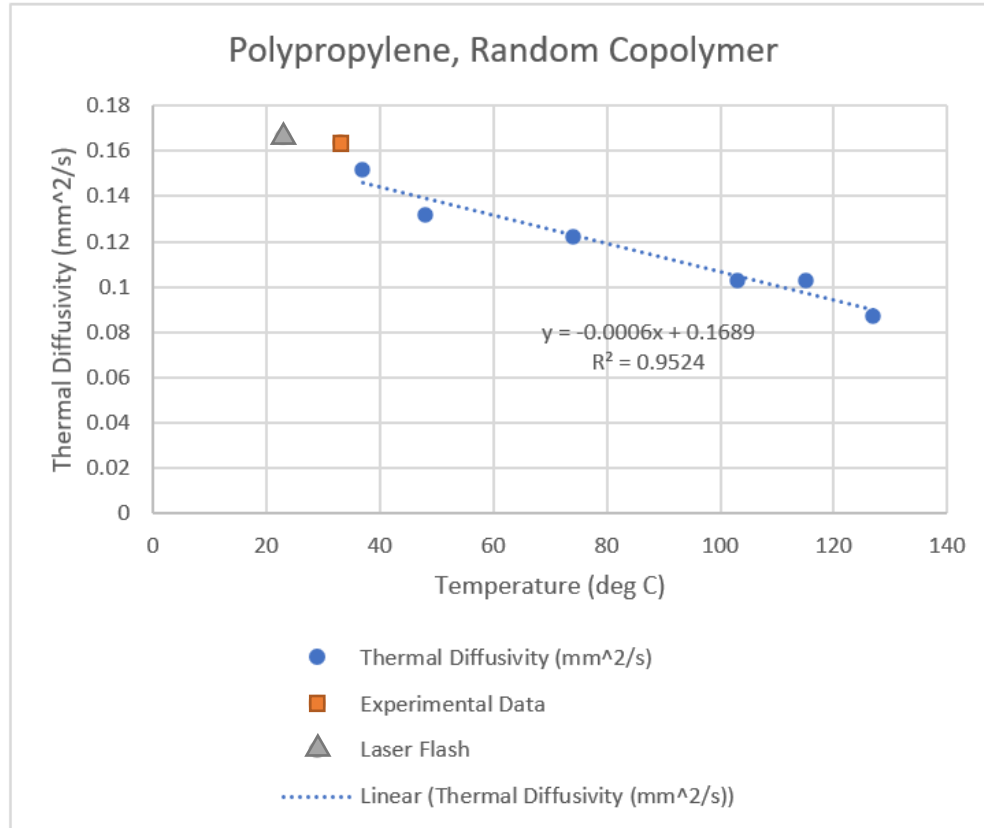


Figure 45 - Curve fit of polypropylene thermal diffusivity data from Zhang and Fujii [14] with experimentally determined and laser flash analysis values overlaid

Using the linear curve fit found, the extrapolated value of thermal diffusivity at 33 deg C is 0.149 mm<sup>2</sup>/s. From this, it is determined that the experimentally found value is ~110% of the value extrapolated from published data. This is sufficiently close to be considered a good result, especially considering the difficulties in measuring thermal diffusivity of low conductivity materials.

Laser flash analysis was completed in the lab using a Netzsch HyperFlash LFA 467 to find the through-plane thermal diffusivity of the virgin polypropylene material. This through-plane thermal diffusivity should be the same as the in-plane thermal diffusivity since the material is isotropic.

Measurement of the sample using laser flash method gave a thermal diffusivity of 0.166-0.167 at ~23° C. Comparing this value from laser flash analysis to the published data, the diffusivity is ~107% of the value extrapolated from published data (which is 0.1551 mm<sup>2</sup>/s at 23° C). Using these sources in combination, it is proven that the experimental setup produces accurate results matching known values.

### **6.2.2 PLA samples**

While the main benefit of analyzing the PLA samples was learning about the importance of a smooth surface texture, the average value for thermal diffusivity found can be compared to published values regardless to determine whether they are approximately what one would expect. Note that the specific filament formulation is unknown beyond knowing the base polymer is polylactic acid, so values are approximate at best. 0.125 mm<sup>2</sup>/s is the experimentally determined average thermal diffusivity from the new setup of Angstrom method using an infrared camera. One group (Zmeskal et al.) found the thermal diffusivity of their PLA samples to be only 0.058 mm<sup>2</sup>/s [17]. Spinelli et al. found the thermal conductivity of neat PLA for 3D printing as 0.183 W/mK, and if the same density and specific heat are used as were used in Zmeskal et al.'s group, the thermal diffusivity comes out to 0.082 mm<sup>2</sup>/s [18]. While the experimentally determined values are significantly higher than those published in these two locations, they are within the correct range of values to be reasonable, especially since additives and pigments in the filament are likely to change thermal diffusivity from the normal value.

### **6.3 Sources of error**

While this infrared camera-based method has produced decent results, there are significant sources of error present in every measurement.



First, measurement point placement in the ResearchIR software is dependent on the camera resolution, and each point must be placed on an exact pixel. This means the measurement point can only get within 0.5 pixel of the exact point to be measured, and there is almost always error present in the results (up to ~0.1mm maximum misalignment). Error in the calculated diffusivity from this issue will also increase as the measurement points used to calculate are placed closer together, since a reduction in distance causes any discrepancy in distance to have a stronger effect.

Next, the infrared camera itself is inherently less accurate than thermocouples and similar physically linked temperature measurement techniques because the camera feed data has much more noise than the thermocouple data. As a reminder, this increased noise with comparison to the signal amplitude can be seen in the discussion of the curve fit approximation process (in particular, Figure 33) This may be due in part to the complexity of the “air gap” between the sample and the camera, since infrared emissions must come from the heated sample, through the viewport of the vacuum chamber, through air, and then into the lens of the camera before finally reaching the microbolometer (sensor). The microbolometer itself has a known noise, given by the Noise Equivalent Temperature Difference (NETD) of the camera, of 0.05 deg C – this defines one standard deviation of the data gathered [5], [19]. The camera also has 76800 points (pixels) which it is measuring the temperature of simultaneously, around 30 times a second, so expecting perfect accuracy at a given individual point is likely outside the scope of the equipment [5]. However, the data analysis performed reduces the effects of these fluctuations almost entirely, since the noise is removed in this data analysis. For measurement points with a high amplitude of the heat sinusoid compared to the amplitude of the noise (at least 2x or 3x the noise amplitude), the noise is of little to no concern. However, below this amplitude, the noise will likely significantly affect the curve fit in analysis, and therefore affect the outcome. It is for this reason that a stronger amplitude heat

wave or points closer to the heater should be used. Another trend can be noticed in the data which supports this decision – calculation values often climb or fall at a consistent slope as the points examined move away from the center. It is believed this is because of the outermost point being the most inaccurate. The outermost points have the lowest amplitude and therefore are approximated with less accuracy than the other points. Thus, as calculations are done using those points, the calculations are pushed either high or low. It is believed the centermost values—those calculated from the points only 2 and 4 mm from the heater edge, respectively—are generally the most accurate calculations.

While these two points (pixel-perfect placement and inherent noise) are the primary sources of error in this method, there are several other possible sources of minor error. Radiative heat transfer is not accounted for, though some thermal energy is of course lost to radiation. Another source of minor error is that the camera keystone, present due to the short focal length, causes very slight distortion of the camera image, and this can cause the reference datum points to not scale perfectly with the sample centerline. Finally, the higher order harmonic of the curve fit is not accounted for since its amplitude is relatively low compared to the main sinusoidal component. Each of these sources contributes some amount of error to the result, but their effect on the outcome is likely small enough to neglect.

A calculation of bias uncertainty was completed for the polypropylene thermal diffusivity measurement using standard techniques, and the average uncertainty calculated was approximately  $0.0227 \text{ mm}^2/\text{s}$ , or roughly 10% of the measured thermal diffusivity [20].

## **Chapter 7: Conclusion and Remarks**

In conclusion, the method to measure thermal diffusivity using Angstrom method with an infrared camera has been developed and tested, and the method offers fairly accurate results while having significant benefits over prior methods used. From the polypropylene tests, it was determined that the method is fairly accurate. Additional lessons were learned about using the method effectively: from the PLA samples, it was discovered that the surface must be smooth and without significant variation, and from the graphene-polymer samples, it was reaffirmed that defects in the material have strong effects on the resulting thermal diffusivity measurement.

This method will be primarily used in the future to characterize materials' thermal diffusivity as compared to each other, reducing the need for very accurate single temperature points. However, the accuracy of measurements taken should be high regardless of this.

### **7.1 Reliability of method**

Now that the method and experimental setup have been put in place, very few adjustments need to be made over time. Preparation of samples and loading of the samples is straightforward, and the camera setup does not require any specific readjustment. There are few things which can go wrong with the setup short of catastrophic failure, so the method should be very reliable.

### **7.2 Future applications of the method**

This method of measuring thermal diffusivity is particularly good for homogenous materials, isotropic materials, and materials with fairly low thermal conductivity. Also, materials must be able to be cut or machined to the required sample dimensions. However, it has been determined that the method is not particularly good for samples with rough or uneven surfaces, any sample

with serious defects or other non-aligned anisotropies, or for any nonplanar samples which do not meet geometry requirements. Materials with very high thermal conductivity may also be a poor choice for this method as it stands, since the 3D printed sample stage is susceptible to damage from samples which become hotter than the melting temperature of PLA out at the ends of the sample, and higher temperatures will likely need to be used for analysis of those higher-conductivity materials.

This method should be ideal for characterizing new materials such as polymer-based nanocomposites, especially when comparing in-plane thermal conductivity to through-plane thermal conductivity obtained via other methods.

### **7.3 Future improvements**

There are a few possible improvements which could be considered for future development of this method:

- More accurate camera, specifically one which produces less noise and has a better microbolometer
- Closer “zoom” lens to reduce error in cursor placement
- Using “cursors” within FLIR ResearchIR which average several points along a line rather than considering only single points – this could reduce noise by averaging data from the beginning.

Overall, the newly developed method of using Angstrom method to measure thermal diffusivity using an infrared camera has been successful and has sufficiently met the goals set forth.

## References

- [1] F. Tarannum, “Effect of Alignment on Thermal Conductivity of Polyethylene-Graphene Composites and Comparison with Effective Medium Theory,” University of Oklahoma, Norman, Oklahoma, 2019.
- [2] M. Wolff, “Measuring Thermal Conductivity by °Angstrom’s Method,” p. 5, May 2016.
- [3] “Arctic Silver Thermal Adhesive.” [http://www.arcticsilver.com/arctic\\_silver\\_thermal\\_adhesive.htm](http://www.arcticsilver.com/arctic_silver_thermal_adhesive.htm) (accessed Apr. 06, 2021).
- [4] R. Franke and A. Kesselboth, “How thin can a sample be?,” May 19, 2017.
- [5] “FLIR A300 (30Hz) Thermal Imaging Camera.” <https://www.oemcameras.com/flir-a-series-a300.htm> (accessed Apr. 08, 2021).
- [6] “FLIR T197215 Close-up Lens with Case for the T4XX Series, 4x.” <https://www.flir-direct.com/product/flir-t197215-close-up-lens-4x> (accessed Apr. 06, 2021).
- [7] T. Hattori, Y. Homma, A. Mitsuishi, and M. Tacke, “Indices of refraction of ZnS, ZnSe, ZnTe, CdS, and CdTe in the far infrared,” *Optics Communications*, vol. 7, no. 3, pp. 229–232, Mar. 1973, doi: 10.1016/0030-4018(73)90015-1.
- [8] Y. Pan, L. Hang, Z. Wu, and Y. Yin, “Design and fabrication of ultra broadband infrared antireflection hard coatings on ZnSe in the range from 2 to 16 $\mu$ m,” *Infrared Physics & Technology*, vol. 52, no. 5, pp. 193–195, Sep. 2009, doi: 10.1016/j.infrared.2009.07.006.
- [9] C. R. Dalton, “Improvements in Scanning Infrared Thermography,” 2010, Accessed: Nov. 04, 2020. [Online]. Available: <https://shareok.org/handle/11244/318872>
- [10] R. E. Drumright, P. R. Gruber, and D. E. Henton, “Polylactic Acid Technology,” *Advanced Materials*, vol. 12, no. 23, pp. 1841–1846, 2000, doi: [https://doi.org/10.1002/1521-4095\(200012\)12:23<1841::AID-ADMA1841>3.0.CO;2-E](https://doi.org/10.1002/1521-4095(200012)12:23<1841::AID-ADMA1841>3.0.CO;2-E).
- [11] D. Garlotta, “A Literature Review of Poly(Lactic Acid),” *Journal of Polymers and the Environment*, vol. 9, no. 2, pp. 63–84, 2001, doi: 10.1023/A:1020200822435.
- [12] A. Azmi, K. Y. Lau, N. A. Ahmad, Z. Abdul-Malek, and W. A. W. A. Rahman, “Thermal and Breakdown Properties of Polypropylene Homopolymer, Copolymer, and Blend,” in *2018 IEEE 7th International Conference on Power and Energy (PECon)*, Dec. 2018, pp. 107–110. doi: 10.1109/PECON.2018.8684178.
- [13] X. Zhang, W. Hendro, M. Fujii, T. Tomimura, and N. Imaishi, “Measurements of the Thermal Conductivity and Thermal Diffusivity of Polymer Melts with the Short-Hot-Wire Method,” *International Journal of Thermophysics*, vol. 23, pp. 1077–1090, Jan. 2002, doi: 10.1023/A:1016394104244.
- [14] X. Zhang and M. Fujii, “Measurements of the thermal conductivity and thermal diffusivity of polymers,” *Polymer Engineering & Science*, vol. 43, no. 11, pp. 1755–1764, 2003, doi: <https://doi.org/10.1002/pen.10148>.

- [15] A. Patti and D. Acierno, "Thermal Conductivity of Polypropylene-Based Materials," *Polypropylene - Polymerization and Characterization of Mechanical and Thermal Properties*, Feb. 2019, doi: 10.5772/intechopen.84477.
- [16] P. Dashora and G. Gupta, "On the temperature dependence of the thermal conductivity of linear amorphous polymers," *Polymer*, vol. 37, no. 2, pp. 231–234, Jan. 1996, doi: 10.1016/0032-3861(96)81092-5.
- [17] O. Zmeskal, L. Marackova, T. Lapcikova, P. Mencik, and R. Prikryl, "Thermal properties of samples prepared from polylactic acid by 3D printing," Smolenice, Slovakia, 2020, p. 020022. doi: 10.1063/5.0033857.
- [18] G. Spinelli *et al.*, "Nanocarbon/Poly(Lactic) Acid for 3D Printing: Effect of Fillers Content on Electromagnetic and Thermal Properties," *Materials*, vol. 12, no. 15, Art. no. 15, Jan. 2019, doi: 10.3390/ma12152369.
- [19] G. Orlove, "IR InformIR Blog: What does Sensitivity (NETD) mean when applied to a Thermal Imager?," *IR InformIR Blog*, Aug. 18, 2017. <http://irinformir.blogspot.com/2017/08/what-does-sensitivity-netd-mean-when.html> (accessed Apr. 29, 2021).
- [20] R. J. Moffat, "Describing the uncertainties in experimental results," *Experimental Thermal and Fluid Science*, vol. 1, no. 1, pp. 3–17, Jan. 1988, doi: 10.1016/0894-1777(88)90043-X.

# Appendix

FLIR Camera output scaler.xlsx – calculations to place six measurement points are completed using equations in cells.

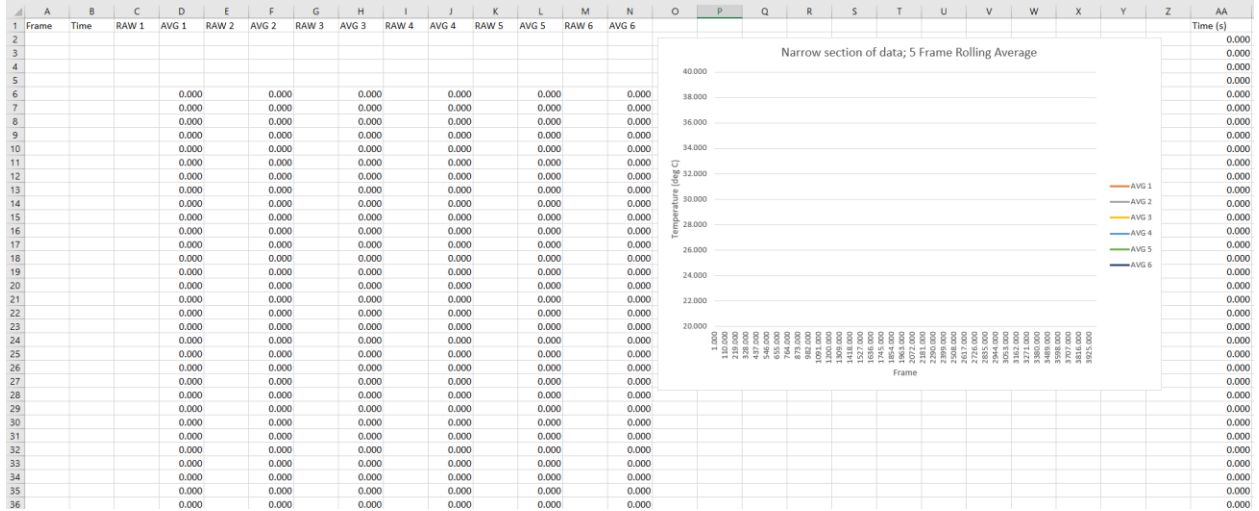
	A	B	C	D	E	F	G	H	I	J	K
1	Reference distance, actual (mm)	14.5	*14.5 top, 15.0 bottom	scale =	0.099962	mm/px					
2											
3	INPUT FROM CAMERA FEED										
4	Ax	87									
5	Ay	166		$\Delta$ pixels in x	$\Delta$ pixels in y	scale length (px)					
6	Bx	232		145	-4	145.0552					
7	By	162									
8	Sample's Y positions at FOV edge		Camera FOV = 360x240px								
9	Cy	78		MPLy	120.5						
10	Dy	163		MPrY	113						
11	Ey	72		m(omega)	-0.0208333	slope of line (mm/mm) rise/run					
12	Fy	154		b(omega)	120.5						
13	Heater edges										
14	Gx	152									
15	Gy	87	L	mGH	550000	slope of line (mm/mm) rise/run					
16	Hx	152.0001		bGH	-83599913						
17	Hy	142	R								
18	Ix	167									
19	Iy	86	L	mIJ	19.333333	slope of line (mm/mm) rise/run					
20	Jx	170		bIJ	-3142.6667						
21	Jy	144	R								
22											
23											
24	Points of intersection										
25	alpha			x(alpha) = x(Omega)GH	152.00006						
26				y(alpha) = y(Omega)GH	117.33333						
27	beta			x(beta) = x(Omega)IJ	168.6028						
28				y(beta) = y(Omega)IJ	116.98744						
29											
30											

	A	B	C	D	E	F	G	H	I	J	K	L
29												
30												
31	d1	-6	mm	d1scaled	-60.022826	px						
32	d2	-4	mm	d2scaled	-40.015217	px						
33	d3	-2	mm	d3scaled	-20.007609	px						
34	d4	2	mm	d4scaled	20.007609	px						
35	d5	4	mm	d5scaled	40.015217	px						
36	d6	6	mm	d6scaled	60.022826	px						
37	(theta)	1.591627	radians									
38												
39	OUTPUT COORDINATES Place measuring points on each of the below (equivalent to where the thermocouples would have been)											
40		x	y									
41	Point 1	91.990	118.584									
42	Point 2	111.994	118.167									
43	Point 3	131.997	117.750									
44	Point 4	188.606	116.571									
45	Point 5	208.609	116.154									
46	Point 6	228.613	115.737									
47												
48												
49												

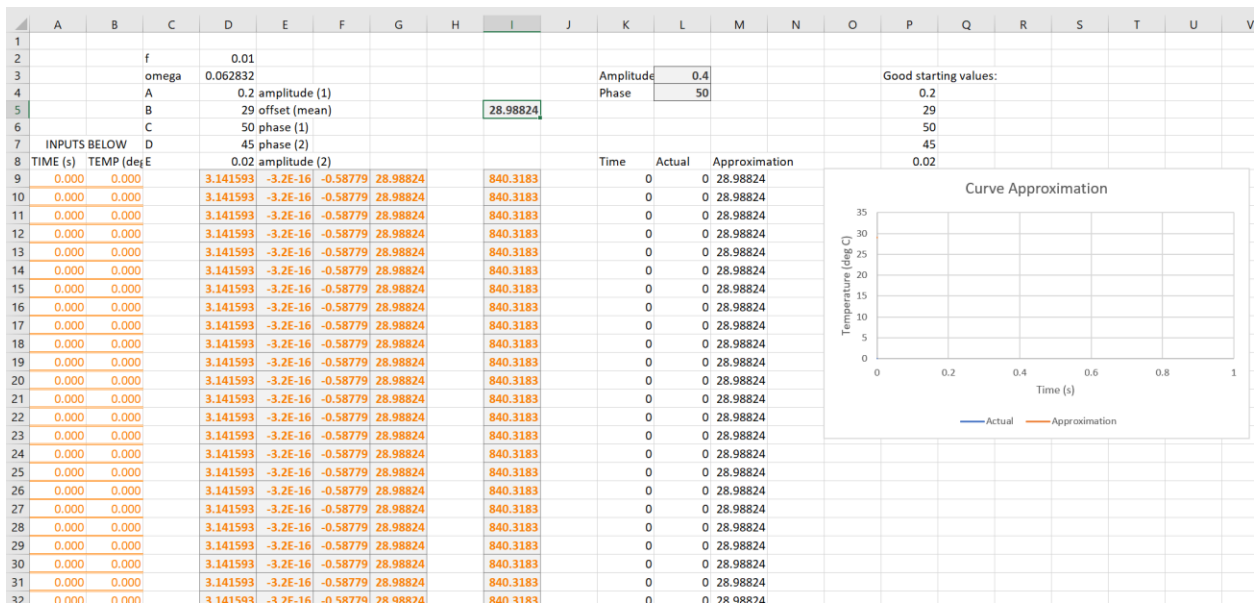
**OUTPUT TO LEFT**

Data Analysis Macro v8 6pt Template.xlsm contents are necessary to use the automated program, specifically the Solver, Results, and Narrow sheets. VBA macros/code are provided below following screenshots of the necessary spreadsheets.

Narrow (continues downward around 4000 rows):



Solver\_1, which is duplicated as Solver\_2 through Solver\_6 (continues downward around 4000 rows):



Results (duplicate calculations are completed for the remaining four combinations of points, and a chart is present):



	A	B	C	D	E	F	G	H	I	J	K	L	M	N	O	P
1	Thermal Conductivity, k (W/mK)		Thermal Diffusivity, alpha (mm <sup>2</sup> /s)													
2	1 to 2	0.1763		0.1009												
3	1 to 3	0.1846		0.1057												
4	2 to 3	0.1949		0.1115												
5	4 to 5	0.1949		0.1115												
6	4 to 6	0.1846		0.1057												
7	5 to 6	0.1763		0.1009												
8																
9																
10																
11																
12	<b>For Cursors 1 &amp; 3</b>					<b>For Cursors 2 &amp; 3</b>										
13	Ratio of amplitudes (3/1)		11.5							Ratio of amplitudes (3/2)		3.06666667				
14	phase difference (s) (3-1)		31							phase difference (s) (3-2)		16				
15																
16	L (mm)		4	distance between temp sensors						L (mm)		2	distance between temp sensors			
17	L (m)		0.004	above distance converted to meters						L (m)		0.002	above distance converted to meters			
18	dt (s)		31	phase difference between two temperature responses						dt (s)		16	phase difference between two temperature responses			
19	M (deg C)		4.6	amplitude of cursor closest to the heater (3)						M (deg C)		4.6	amplitude of cursor closest to the heater (3)			
20	N (deg C)		0.4	amplitude of cursor further away from the heater (1)						N (deg C)		1.5	amplitude of cursor further away from the heater (2)			
21	alpha (m <sup>2</sup> /s)		1.05663E-07	thermal diffusivity						alpha (m <sup>2</sup> /s)		1.11548E-07	thermal diffusivity			
22																
23	rho (kg/m <sup>3</sup> )		910	density (applied to all conductivity calculations)												
24	Cp (J/K*kg)		1920	specific heat (applied to all conductivity calculations)												
25	k (W/mK)		0.184613536	thermal conductivity						k (W/mK)		0.194897123	thermal conductivity			
26																
27																
28																

Theory behind Solver portion:

03/22/2021

$$A \cdot \sin(\omega \cdot (t+C)) + B + E \cdot \left( \sin(2\omega(t+D)) \right) = \Theta = \text{approximation of curve (datapoint)}$$

Error:  $(\text{Temp} - \Theta)^2 = \text{Error}(t)$   $n_{pt} = \text{num. of data points}$

FINAL: ~~XXXXXXXXXX~~  $\left( \frac{\sum_{t=1}^{n_{pt}} (\text{Error}(t))}{n_{pt}} \right)^{1/2}$  ← goal: minimize this by setting A, B, C, D, E with a numerical method solver.

(least squares method)

A =  $\left(\frac{1}{2}\right)$  amplitude of first sine wave  
 B = offset (mean level)  
 C = phase of sine wave #1  
 D = phase of sine wave #2  
 E = amplitude of second sine wave  
 (1/2?)

Program/Macro code for all subroutines of Data Analysis Macro v8 6pt Template.xlsm follow:

```
Sub InitialPull()
'
' InitialPull Macro
' pull in data from the other sheets
```

```
'  
' 6 cursor version 03/25/2021
```

```
Dim mainWbName As String
```

```
mainWbName = ActiveWorkbook.Name
```

```
Application.ScreenUpdating = False
```

```
Windows("Cursor 1.csv").Activate  
Sheets("Cursor 1").Select  
Sheets("Cursor 1").Copy After:=Workbooks(mainWbName).Sheets(2)  
Windows("Cursor 2.csv").Activate  
Sheets("Cursor 2").Select  
Sheets("Cursor 2").Copy After:=Workbooks(mainWbName).Sheets(3)  
Windows("Cursor 3.csv").Activate  
Sheets("Cursor 3").Select  
Sheets("Cursor 3").Copy After:=Workbooks(mainWbName).Sheets(4)  
Windows("Cursor 4.csv").Activate  
Sheets("Cursor 4").Select  
Sheets("Cursor 4").Copy After:=Workbooks(mainWbName).Sheets(5)  
Windows("Cursor 5.csv").Activate  
Sheets("Cursor 5").Select  
Sheets("Cursor 5").Copy After:=Workbooks(mainWbName).Sheets(6)  
Windows("Cursor 6.csv").Activate  
Sheets("Cursor 6").Select  
Sheets("Cursor 6").Copy After:=Workbooks(mainWbName).Sheets(7)
```

```
Windows("Cursor 1.csv").Activate  
ActiveWindow.Close  
Windows("Cursor 2.csv").Activate  
ActiveWindow.Close  
Windows("Cursor 3.csv").Activate  
ActiveWindow.Close  
Windows("Cursor 4.csv").Activate  
ActiveWindow.Close  
Windows("Cursor 5.csv").Activate  
ActiveWindow.Close  
Windows("Cursor 6.csv").Activate  
ActiveWindow.Close
```

```
Application.ScreenUpdating = True
```

```
Sheets("Instructions").Select
```

End Sub

---

```
Sub CombineDataWChart()  
,  
' CombineDataWChart Macro  
' combining all data into one sheet - uses four sheets to start, one  
for each Cursor data.  
' also creates a chart of all the data using the rolling averages  
,  
' 6 cursor version 03/25/2021  
'MAJOR BUG FIX 03/30/2021 - Cursor data getting copied to new sheet was  
incorrect in all previous 6pt versions. Copied starting at row 2 rather  
than finding firstFrame row  
  
Dim firstFrame As String  
Dim rowFound As Long  
Dim copyRange As String  
Dim lastCursor1Row As Long  
Dim autofillRange As String  
  
Application.ScreenUpdating = False  
  
'MAKE NEW SHEET  
  Sheets("Cursor 6").Select  
  Sheets.Add After:=ActiveSheet  
  Sheets(ActiveSheet.Name).Select  
  Sheets(ActiveSheet.Name).Name = "Combined Data"  
  
'CURSOR DATA - COPY TO NEW SHEET  
  'CURSOR 6  
  Sheets("Cursor 6").Select  
  Range("A2:D2").Select      'select across row - starting with first  
row  
  Range(Selection, Selection.End(xlDown)).Select  
  Application.CutCopyMode = False 'clears out previous copy  
  Selection.Copy  
  Sheets("Combined Data").Select  
  Range("U1").Select      'cursor 6 data location  
  ActiveSheet.Paste  
  
  firstFrame = Range("U1").Value 'pull the first frame number from  
last set of data (cursor 6 here)
```

```

'CURSOR 5
Sheets("Cursor 5").Select
rowFound = ActiveSheet.Range("A:A").Find(What:=firstFrame,
LookIn:=xlValues).Row
Let copyRange = "A" & rowFound & ":" & "D" & rowFound
Range(copyRange).Select

Range(Selection, Selection.End(xlDown)).Select
Application.CutCopyMode = False
Selection.Copy
Sheets("Combined Data").Select
Range("Q1").Select 'cursor 5 data location
ActiveSheet.Paste

'CURSOR 4
Sheets("Cursor 4").Select
rowFound = ActiveSheet.Range("A:A").Find(What:=firstFrame,
LookIn:=xlValues).Row
Let copyRange = "A" & rowFound & ":" & "D" & rowFound
Range(copyRange).Select

Range(Selection, Selection.End(xlDown)).Select
Application.CutCopyMode = False
Selection.Copy
Sheets("Combined Data").Select
Range("M1").Select
ActiveSheet.Paste

'CURSOR 3
Sheets("Cursor 3").Select
rowFound = ActiveSheet.Range("A:A").Find(What:=firstFrame,
LookIn:=xlValues).Row
Let copyRange = "A" & rowFound & ":" & "D" & rowFound
Range(copyRange).Select

Range(Selection, Selection.End(xlDown)).Select
Application.CutCopyMode = False
Selection.Copy
Sheets("Combined Data").Select
Range("I1").Select
ActiveSheet.Paste

'CURSOR 2
Sheets("Cursor 2").Select
rowFound = ActiveSheet.Range("A:A").Find(What:=firstFrame,
LookIn:=xlValues).Row
Let copyRange = "A" & rowFound & ":" & "D" & rowFound
Range(copyRange).Select

```

```

Range(Selection, Selection.End(xlDown)).Select
Application.CutCopyMode = False
Selection.Copy
Sheets("Combined Data").Select
Range("E1").Select
ActiveSheet.Paste

'Cursors 1
Sheets("Cursor 1").Select
rowFound = ActiveSheet.Range("A:A").Find(What:=firstFrame,
LookIn:=xlValues).Row
Let copyRange = "A" & rowFound & ":" & "D" & rowFound
Range(copyRange).Select

Range(Selection, Selection.End(xlDown)).Select
Application.CutCopyMode = False
Selection.Copy
Sheets("Combined Data").Select
Range("A1").Select
ActiveSheet.Paste

'Hide each individual Cursor sheet
Sheets("Cursor 1").Visible = False
Sheets("Cursor 2").Visible = False
Sheets("Cursor 3").Visible = False
Sheets("Cursor 4").Visible = False
Sheets("Cursor 5").Visible = False
Sheets("Cursor 6").Visible = False

'DELETE UNNECESSARY DATA
Range("F16").Select
Application.CutCopyMode = False
Range("C:C,G:G,K:K,O:O,S:S,W:W").Select 'pick out relative time
rows
Range("W1").Activate
Selection.Delete Shift:=xlToLeft
Range("D:D,E:E, G:G,H:H, J:J,K:K, M:M,N:N, P:P,Q:Q,
S:S,T:T").Select 'pick out redundant frame and abs. time rows
Range("T1").Activate
Selection.Delete Shift:=xlToLeft

'Get last row of Cursor 1 data
lastCursor1Row = Cells(Rows.Count, 1).End(xlUp).Row 'finds last row
with data in column A (1)

'ADD (5 FRAMES) ROLLING AVG COLUMNS
Columns("D:D").Select

```

```

    Selection.Insert                               Shift:=xlToRight,
CopyOrigin:=xlFormatFromLeftOrAbove
    Columns("F:F").Select
    Selection.Insert                               Shift:=xlToRight,
CopyOrigin:=xlFormatFromLeftOrAbove
    Columns("H:H").Select
    Selection.Insert                               Shift:=xlToRight,
CopyOrigin:=xlFormatFromLeftOrAbove
    Columns("J:J").Select
    Selection.Insert                               Shift:=xlToRight,
CopyOrigin:=xlFormatFromLeftOrAbove
    Columns("L:L").Select
    Selection.Insert                               Shift:=xlToRight,
CopyOrigin:=xlFormatFromLeftOrAbove

```

```

'initial rolling avg setup
Range("D5").Select
ActiveCell.FormulaR1C1 = "=SUM(R[-4]C[-1]:RC[-1]) / 5" 'takes
average data value of 5 points, starting with 4 rows above current
Range("D5").Select

```

```

Let autofillRange = "D5:" & "D" & lastCursor1Row
Selection.AutoFill Destination:=Range(autofillRange)

```

```

'copy column to other locations
Columns("D:D").Select
Selection.Copy
Columns("F:F").Select
ActiveSheet.Paste
Columns("H:H").Select
ActiveSheet.Paste
Columns("J:J").Select
ActiveSheet.Paste
Columns("L:L").Select
ActiveSheet.Paste
Columns("N:N").Select
ActiveSheet.Paste
Application.CutCopyMode = False 'clear out selection

```

```

'ADD HEADER ROW
Rows("1:1").Select
Selection.Insert                               Shift:=xlDown,
CopyOrigin:=xlFormatFromLeftOrAbove

```

```

Range("A1").Select
ActiveCell.FormulaR1C1 = "Frame"
Range("B1").Select
ActiveCell.FormulaR1C1 = "Time"
Range("C1").Select

```

```

ActiveCell.FormulaR1C1 = "RAW 1"
Range("D1").Select
ActiveCell.FormulaR1C1 = "AVG 1"
Range("E1").Select
ActiveCell.FormulaR1C1 = "RAW 2"
Range("F1").Select
ActiveCell.FormulaR1C1 = "AVG 2"
Range("G1").Select
ActiveCell.FormulaR1C1 = "RAW 3"
Range("H1").Select
ActiveCell.FormulaR1C1 = "AVG 3"
Range("I1").Select
ActiveCell.FormulaR1C1 = "RAW 4"
Range("J1").Select
ActiveCell.FormulaR1C1 = "AVG 4"
Range("K1").Select
ActiveCell.FormulaR1C1 = "RAW 5"
Range("L1").Select
ActiveCell.FormulaR1C1 = "AVG 5"
Range("M1").Select
ActiveCell.FormulaR1C1 = "RAW 6"
Range("N1").Select
ActiveCell.FormulaR1C1 = "AVG 6"

' remove excess/junk data from end
Rows(lastCursor1Row & ":" & Rows.Count).Delete
'could have also used the Range.Find method

' put in General format with 3 decimal places
Range("C2:N" & lastCursor1Row).Select
Selection.NumberFormat = "General"
Selection.NumberFormat = "0.000"

' ADDING CHART
Range("L1").Select
ActiveSheet.Shapes.AddChart2(227, xlLine).Select
ActiveSheet.Shapes("Chart 1").IncrementLeft 350
ActiveSheet.Shapes("Chart 1").IncrementTop -120
ActiveSheet.Shapes("Chart 1").ScaleWidth 1.5, msoFalse, _
    msoScaleFromTopLeft
ActiveSheet.Shapes("Chart 1").ScaleHeight 1.55, msoFalse, _
    msoScaleFromTopLeft
Application.CutCopyMode = False
ActiveChart.SetSourceData
Source:=Range("D:D,F:F,H:H,J:J,L:L,N:N,B:B")

'set title
ActiveSheet.ChartObjects("Chart 1").Activate
ActiveChart.chartTitle.Select

```

```

ActiveChart.chartTitle.Text = "Full Combined Data; 5 Frame Rolling
Average"
Selection.Format.TextFrame2.TextRange.Characters.Text = _
    "Full Combined Data; 5 Frame Rolling Average"
With Selection.Format.TextFrame2.TextRange.Characters(1,
43).ParagraphFormat
    .TextDirection = msoTextDirectionLeftToRight
    .Alignment = msoAlignCenter
End With

'add legend and change y scale minimum to 20 degrees C
ActiveChart.Axes(xlValue).Select
ActiveChart.Axes(xlValue).MinimumScale = 20
ActiveChart.SetElement (msoElementLegendRight)

Application.ScreenUpdating = True

End Sub

```

---

```

Sub NarrowData()
'
' NarrowData Macro
' pulls from Combined Data sheet into the Narrow sheet
'
' 6 cursor version

Dim StartRowNum, EndRowNum As Long
Dim copyRange As String

'
    Sheets("Combined Data").Select

StartRowNum = Cells(Rows.Count, 1).End(xlUp).Row - 6000 'sets to row
6000 from bottom
EndRowNum = Cells(Rows.Count, 1).End(xlUp).Row - 2000 'sets to row 2000
from bottom

Application.ScreenUpdating = False

```



```

'take the frame and time columns
  Let copyRange = "A" & StartRowNum & ":" & "A" & EndRowNum 'now
selects specific section of data
  Range(copyRange).Select
  'Range(Selection, Selection.End(xlDown)).Select 'snap to end of
data
  Selection.Copy
  Sheets("Narrow").Select
  Range("A2").Select
  ActiveSheet.Paste
  Sheets("Combined Data").Select
  Application.CutCopyMode = False

  Let copyRange = "B" & StartRowNum & ":" & "B" & EndRowNum
  Range(copyRange).Select
  'Range(Selection, Selection.End(xlDown)).Select 'snap to end of
data
  Selection.Copy
  Sheets("Narrow").Select
  Range("B2").Select
  ActiveSheet.Paste
  Sheets("Combined Data").Select
  Application.CutCopyMode = False

'pull in raw data for each point
  Let copyRange = "C" & StartRowNum & ":" & "C" & EndRowNum
  Range(copyRange).Select
  'Range(Selection, Selection.End(xlDown)).Select
  Selection.Copy
  Sheets("Narrow").Select
  Range("C2").Select
  ActiveSheet.Paste
  Sheets("Combined Data").Select
  Application.CutCopyMode = False

  Let copyRange = "E" & StartRowNum & ":" & "E" & EndRowNum
  Range(copyRange).Select
  'Range(Selection, Selection.End(xlDown)).Select
  Selection.Copy
  Sheets("Narrow").Select
  Range("E2").Select
  ActiveSheet.Paste
  Sheets("Combined Data").Select
  Application.CutCopyMode = False

  Let copyRange = "G" & StartRowNum & ":" & "G" & EndRowNum
  Range(copyRange).Select
  'Range(Selection, Selection.End(xlDown)).Select
  Selection.Copy

```

```
Sheets("Narrow").Select
Range("G2").Select
ActiveSheet.Paste
Sheets("Combined Data").Select
Application.CutCopyMode = False
```

```
Let copyRange = "I" & StartRowNum & ":" & "I" & EndRowNum
Range(copyRange).Select
'Range(Selection, Selection.End(xlDown)).Select
Selection.Copy
Sheets("Narrow").Select
Range("I2").Select
ActiveSheet.Paste
Sheets("Combined Data").Select
Application.CutCopyMode = False
```

```
Let copyRange = "K" & StartRowNum & ":" & "K" & EndRowNum
Range(copyRange).Select
'Range(Selection, Selection.End(xlDown)).Select
Selection.Copy
Sheets("Narrow").Select
Range("K2").Select
ActiveSheet.Paste
Sheets("Combined Data").Select
Application.CutCopyMode = False
```

```
Let copyRange = "M" & StartRowNum & ":" & "M" & EndRowNum
Range(copyRange).Select
'Range(Selection, Selection.End(xlDown)).Select
Selection.Copy
Sheets("Narrow").Select
Range("M2").Select
ActiveSheet.Paste
Sheets("Combined Data").Select
Application.CutCopyMode = False
```

```
'go back to combined data and focus on top corner
Sheets("Combined Data").Select 'redundant sheet selection, just to
make sure.
```

```
Range("A1").Select
```

```
'move new Time column into place
Sheets("Narrow").Select
Columns("AA:AA").Select
Selection.Cut
Columns("C:C").Select
Selection.Insert Shift:=xlToRight
Range("A1").Select
Sheets("Narrow").Select
```

```
Application.ScreenUpdating = True
```

```
End Sub
```

---

```
Sub SolverRunV2()  
,  
,  
, SolverRunV2 Macro  
,  
,  
, to make this run, you must go to the Visual Basic editor (you're  
probably already there) > Tools > References > check the "Solver" box.  
,  
, 6 cursor version.  
,  
  
    Sheets("Solver_1").Select 'go to solver 1 sheet  
    Range("I5").Select      'likely unnecessary  
    SolverReset  
    SolverOk      SetCell:="$I$5",      MaxMinVal:=2,      ValueOf:=0,  
ByChange:="$D$4:$D$8", _  
    Engine:=1, EngineDesc:="GRG Nonlinear" 'set parameters  
    SolverSolve True      'runs solver - "true" argument prevents  
the confirmation box from showing up  
  
    Sheets("Solver_2").Select  
    Range("I5").Select  
    SolverReset  
    SolverOk      SetCell:="$I$5",      MaxMinVal:=2,      ValueOf:=0,  
ByChange:="$D$4:$D$8", _  
    Engine:=1, EngineDesc:="GRG Nonlinear"  
    SolverSolve True  
  
    Sheets("Solver_3").Select  
    Range("I5").Select  
    SolverReset  
    SolverOk      SetCell:="$I$5",      MaxMinVal:=2,      ValueOf:=0,  
ByChange:="$D$4:$D$8", _  
    Engine:=1, EngineDesc:="GRG Nonlinear"  
    SolverSolve True  
  
    Sheets("Solver_4").Select  
    Range("I5").Select
```

```

    SolverReset
    SolverOk      SetCell:="$I$5",      MaxMinVal:=2,      ValueOf:=0,
ByChange:="$D$4:$D$8", _
      Engine:=1, EngineDesc:="GRG Nonlinear"
    SolverSolve True

    Sheets("Solver_5").Select
    Range("I5").Select
    SolverReset
    SolverOk      SetCell:="$I$5",      MaxMinVal:=2,      ValueOf:=0,
ByChange:="$D$4:$D$8", _
      Engine:=1, EngineDesc:="GRG Nonlinear"
    SolverSolve True

    Sheets("Solver_6").Select
    Range("I5").Select
    SolverReset
    SolverOk      SetCell:="$I$5",      MaxMinVal:=2,      ValueOf:=0,
ByChange:="$D$4:$D$8", _
      Engine:=1, EngineDesc:="GRG Nonlinear"
    SolverSolve True

    Sheets("Results").Select

```

End Sub

---

```
Sub CleanupWB()
```

```
' Clears out the whole workbook, removing the original data input, the
Narrow copied data, and deleting the Combined Data sheet
'
```

```
Application.DisplayAlerts = False 'switching off the confirmation
button
```

```
Sheets("Combined Data").Delete
DeleteOriginalSheets
```

```
Application.DisplayAlerts = True 'switching the confirmation button  
back on
```

```
SolverResetValues 'calls the SolverResetValues macro  
ClearNarrow 'calls the ClearNarrow macro
```

```
Sheets("Instructions").Select
```

```
End Sub
```

---

```
Sub ClearNarrow()  
,
```

```
' ClearNarrow Macro  
' Clean up the narrow sheet and prepare it for the macro to fill it in  
again  
,
```

```
' 6 cursor version 03/25/2021  
,
```

```
Application.ScreenUpdating = False
```

```
Sheets("Narrow").Select  
Range("A2").Select  
Range(Selection, Selection.End(xlDown)).Select  
Selection.ClearContents  
Range("B2").Select  
Range(Selection, Selection.End(xlDown)).Select  
Selection.ClearContents  
Range("D2").Select  
Range(Selection, Selection.End(xlDown)).Select  
Selection.ClearContents  
Range("F2").Select  
Range(Selection, Selection.End(xlDown)).Select  
Selection.ClearContents  
Range("H2").Select  
Range(Selection, Selection.End(xlDown)).Select  
Selection.ClearContents  
Range("J2").Select  
Range(Selection, Selection.End(xlDown)).Select  
Selection.ClearContents  
Range("L2").Select  
Range(Selection, Selection.End(xlDown)).Select  
Selection.ClearContents  
Range("N2").Select  
Range(Selection, Selection.End(xlDown)).Select  
Selection.ClearContents
```

```
Columns("C:C").Select
Selection.Cut
Columns("AB:AB").Select
Selection.Insert Shift:=xlToRight
Range("A1").Select
```

```
Application.ScreenUpdating = True
```

```
End Sub
```

---

```
Sub DeleteOriginalSheets()
```

```
' 6 cursor version
```

```
Application.DisplayAlerts = False 'switching off the confirmation
button
```

```
Application.ScreenUpdating = False
```

```
Sheets("Cursor 1").Delete
```

```
Sheets("Cursor 2").Delete
```

```
Sheets("Cursor 3").Delete
```

```
Sheets("Cursor 4").Delete
```

```
Sheets("Cursor 5").Delete
```

```
Sheets("Cursor 6").Delete
```

```
Application.DisplayAlerts = True 'switching the confirmation button
back on
```

```
Application.ScreenUpdating = True
```

```
End Sub
```

---

```
Sub SolverResetValues()
```

```
' Copy/Pastes the "Good starting values" into the spots for ABCDE in
each Solver sheet.
```

```
' 6 cursor version
```

```
Application.ScreenUpdating = False
```

```

    Sheets("Solver_1").Select
    Range("P4:P8").Select
    Application.CutCopyMode = False 'clears out previous copy if
applicable
    Selection.Copy
    Range("D4:D8").Select
    ActiveSheet.Paste
    Application.CutCopyMode = False
    Range("I5").Select

    Sheets("Solver_2").Select
    Range("P4:P8").Select
    Application.CutCopyMode = False 'clears out previous copy if
applicable
    Selection.Copy
    Range("D4:D8").Select
    ActiveSheet.Paste
    Application.CutCopyMode = False
    Range("I5").Select

    Sheets("Solver_3").Select
    Range("P4:P8").Select
    Application.CutCopyMode = False 'clears out previous copy if
applicable
    Selection.Copy
    Range("D4:D8").Select
    ActiveSheet.Paste
    Application.CutCopyMode = False
    Range("I5").Select

    Sheets("Solver_4").Select
    Range("P4:P8").Select
    Application.CutCopyMode = False 'clears out previous copy if
applicable
    Selection.Copy
    Range("D4:D8").Select
    ActiveSheet.Paste
    Application.CutCopyMode = False
    Range("I5").Select

    Sheets("Solver_5").Select
    Range("P4:P8").Select
    Application.CutCopyMode = False 'clears out previous copy if
applicable
    Selection.Copy
    Range("D4:D8").Select
    ActiveSheet.Paste
    Application.CutCopyMode = False
    Range("I5").Select

```

```
    Sheets("Solver_6").Select
    Range("P4:P8").Select
    Application.CutCopyMode = False 'clears out previous copy if
applicable
    Selection.Copy
    Range("D4:D8").Select
    ActiveSheet.Paste
    Application.CutCopyMode = False
    Range("I5").Select

Application.ScreenUpdating = True

End Sub
```

---

```
Sub TheWholeShebang()
'runs all of the main macros sequentially, to make the whole analysis
happen in one step (assuming it all goes well)

    InitialPull
    CombineDataWChart
    NarrowData
    SolverRunV2

End Sub
```